Jmjd2c/Kdm4c facilitates the assembly of essential enhancer-protein complexes at the onset of embryonic stem cell differentiation

Rute A. Tomaz, Jennifer L. Harman, Donja Karimlou, Lauren Weavers, Lauriane Fritsch, Tony Bou-Kheir, Emma Bell, Ignacio del Valle Torres, Kathy K. Niakan, Cynthia Fisher, Onkar Joshi, Hendrik G. Stunnenberg, Edward Curry, Slimane Ait-Si-Ali, Helle F. Jørgensen and Véronique Azuara

List of Supplementary Material

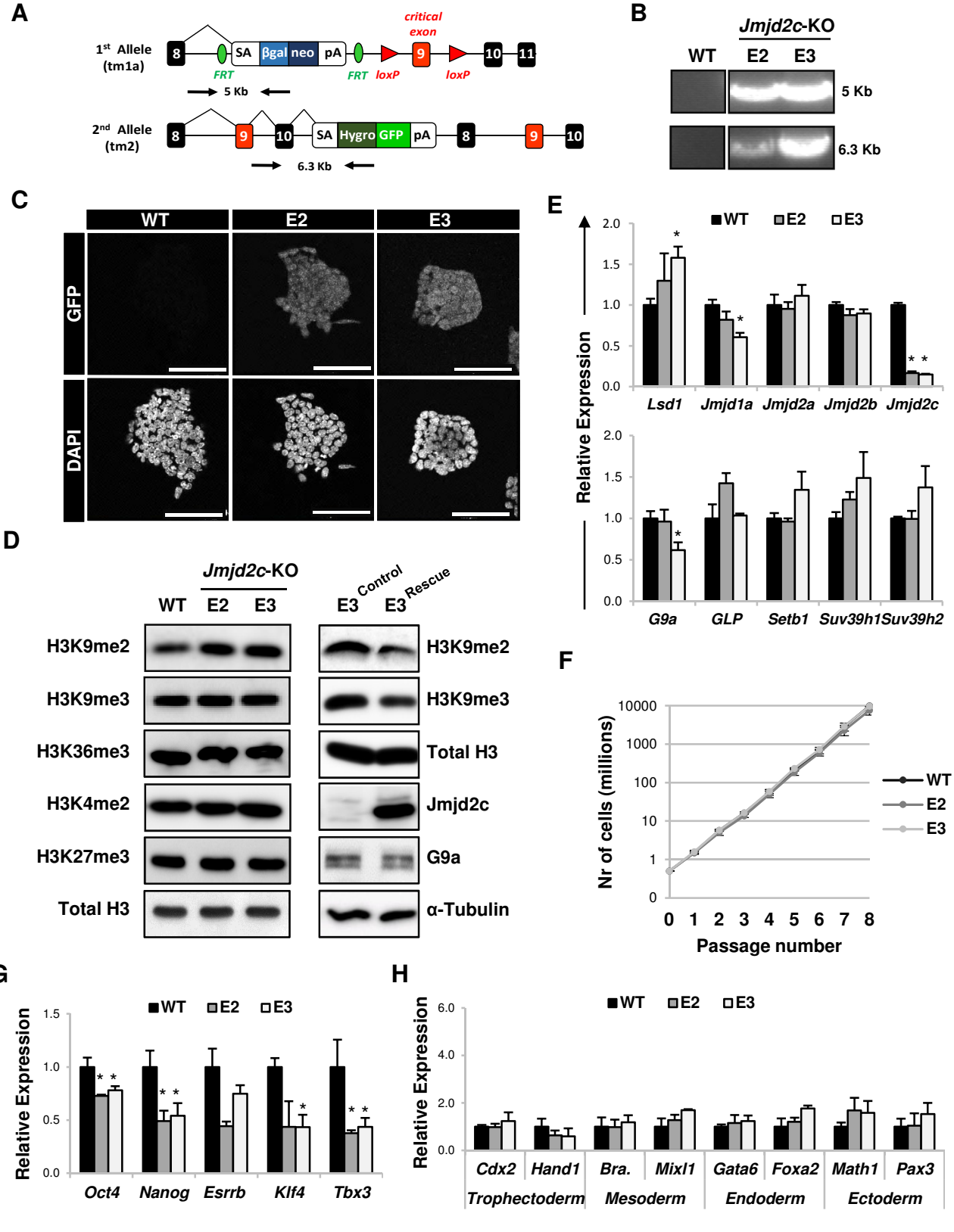

Fig.S1. Validation and characterization of *Jmjd2c*-knockout embryonic stem cell (ESC) clones. (A) Scheme showing *Jmjd2c* targeted alleles. Black boxes indicate exons and red boxes the critical exon 9, white boxes splice acceptor sequences (SA) or polyadenylation sequences (pA), blue (tm1a allele) and green (tm2 allele) boxes drug resistance (neomycin (neo), hygromycin (hyg)) and marker (lacZ and GFP) genes, green circles and red triangles show FRT and loxP sites, respectively. Opposing arrows indicate the position of primer pairs used for genotyping. (B) EtBr agarose gel showing long range PCR products of genomic DNA of wild-type (WT) and homozygous *Jmjd2c*-knockout (*Jmjd2c*-KO) JM8-ESC clones (E2, E3) using primers indicated in (A). Fragment sizes are indicated in kilobases. (C) Anti-GFP labelling and DAPI staining of WT and *Jmjd2c*-KO ESC clones. Bars, 100 µm. (D) Western blot of acid-extracted histone lysates from WT and *Jmjd2c*-KO ESC clones (left panels) showing bulk levels of H3K9me2, H3K9me3, H3K36me3, H3K4me2, H3K27me3 and total H3. Western blot of acid-extracted histone lysates and whole cell extracts of *Jmjd2c*-KO ESC clone E3 transfected with an empty vector (Control) or with full-length *Jmjd2c* cDNA (Rescue) (right panels) showing bulk levels of H3K9me2, H3K9me3 and total H3 (upper lanes), and Jmjd2c, G9a and α-Tubulin (bottom lanes). (E) Relative expression levels of a panel of H3K9-demethylases (upper panel) and H3K9-methyltransferases (bottom panel) in WT and *Jmjd2c*-KO ESC clones grown in serum/LIF. (F) Growth curve of WT (ESC^{WT}) and Jmjd2c-KO ($ESC^{Jmjd2c\text{-}KO}$) clones E2 and E3 in self-renewing conditions over 8 passages (16 days). Plot represents an average of the cell number scored in 3 independent experiments. Error bars indicate ±s.e.m. (G) Relative expression levels of the pluripotency-associated markers *Oct4*, *Nanog*, *Esrrb*, *Klf4* and *Tbx3* in WT and *Jmjd2c*-KO ESC clones. (H) Relative expression levels of differentiation markers associated to the trophectoderm (*Cdx2* and *Hand1*), mesoderm (*Brachyury* and *Mixl1*), endoderm (*Gata6* and *Foxa2*) and ectoderm (*Math1* and *Pax3*) lineages in WT and *Jmjd2c*-KO ESC clones. All expression data were normalised to two housekeeping genes, and expressed relative to WT as the mean±s.e.m. of at least three biological replicates. **P*<0.05; Mann-Whitney *U* test.

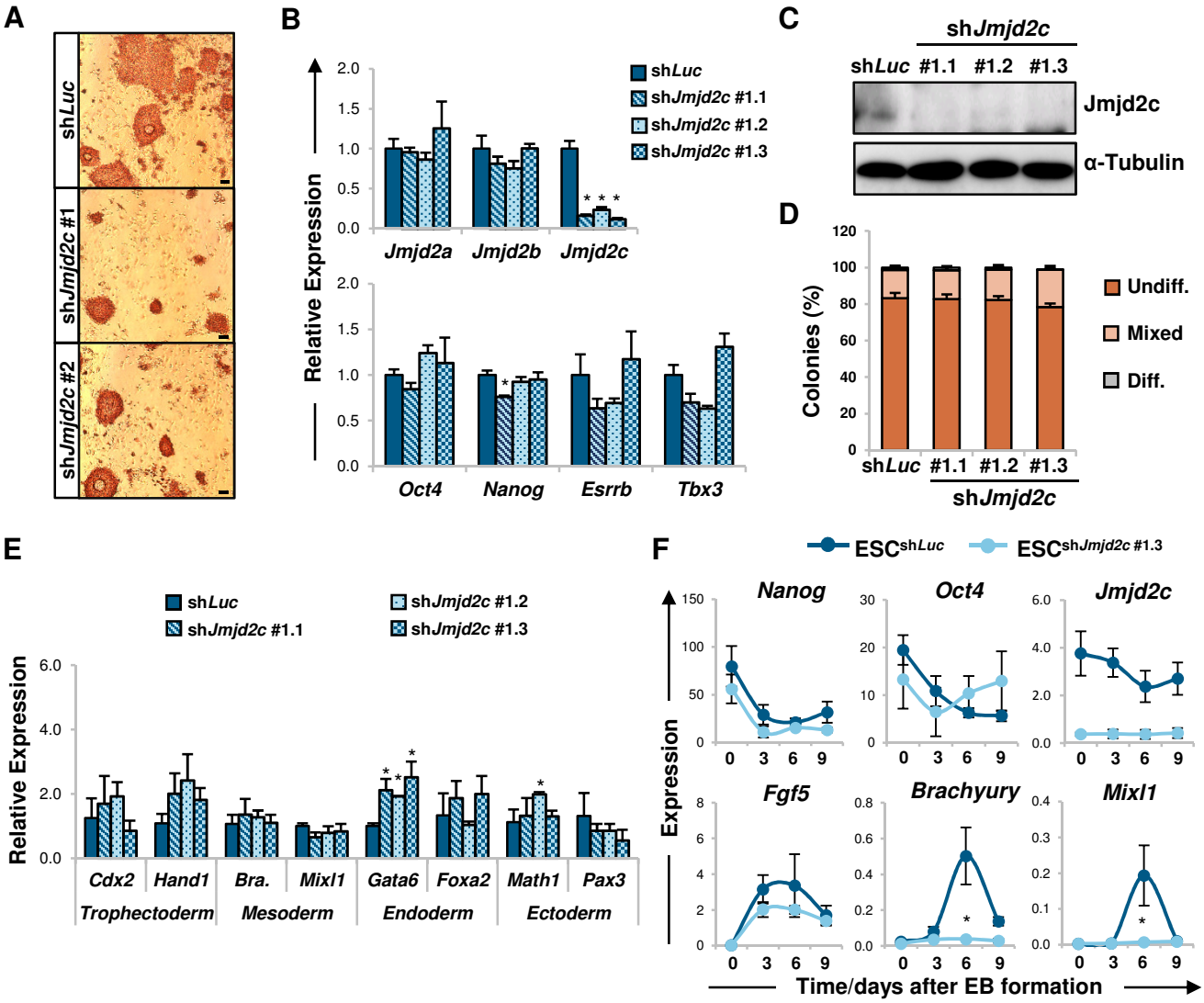

Fig. S2. Generation of embryoid bodies (EBs) is compromised in stable *Jmjd2c*-knockdown ESC clones. (A) E14-ESCs cells were transfected with two independent puromycin-selectable shRNA vectors targeting *Jmjd2c* (sh*Jmjd2c* #1 and #2) or a control vector (sh*Luc*) targeting *Luciferase* (Loh et al., 2007). Selection was maintained for 4 days, then cells were fixed and stained for alkaline phosphatase activity. Bars, 100 µm. (B) Relative expression levels of *Jmjd2* family members and selected pluripotency-associated factors in three stable *Jmjd2c*-knockdown clones established from transfected ESCs with sh*Jmjd2c* #1 vector. Data were normalised to housekeeping genes, and expressed relative to a control ESC clone (sh*Luc*) as mean±s.e.m. of three biological replicates. **P*<0.05; Mann-Whitney *U* test. (C) Western blot using anti-Jmjd2c antibodies on whole cell extracts of three stable *Jmjd2c*-knockdown ESC clones (sh*Jmjd2c* #1.1, #1.2 and #1.3) and a control clone (sh*Luc*). α-Tubulin is used as loading control. (D) Percentage of colonies scored as undifferentiated (Undiff.), mixed or differentiated (Diff.) according to the intensity of alkaline phosphatase staining of stable *Jmjd2c*-knockdown and control ESC clones. Each cell line was plated at low density and cultured for 5 days with LIF and serum. Data are the mean±s.e.m. of three biological replicates. (E) Relative expression levels of differentiation markers associated to the trophectoderm (*Cdx2* and *Hand1*), mesoderm (*Brachyury* and *Mixl1*), endoderm (*Gata6* and *Foxa2*) and ectoderm (*Math1* and *Pax3*) lineages in control (sh*Luc*) and *Jmjd2c*-knockdown (sh*Jmjd2c* #1.1, #1.2 and #1.3) ESC clones. Data were normalised to two housekeeping genes, and expressed relative to a control ESC clone (sh*Luc*) as mean±s.e.m. of three biological replicates. **P*<0.05; Mann-Whitney *U* test. (F) Transcript levels of pluripotency-associated (*Nanog* and *Oct4*), *Jmjd2c*, and early differentiation markers for epiblast (*Fgf5*) and primitive streak (*Brachyury* and *Mixl1*) in sh*Jmjd2c* clone #1.3 and sh*Luc* control ESCs upon EB-induced differentiation. Similar results were obtained in sh*Jmjd2c* clone #1.2 and #1.1 ESCs (data not shown). Data were normalized to two housekeeping genes, and expressed as the mean±s.e.m. of at least three independent experiments. **P*<0.05; Mann-Whitney *U* test.

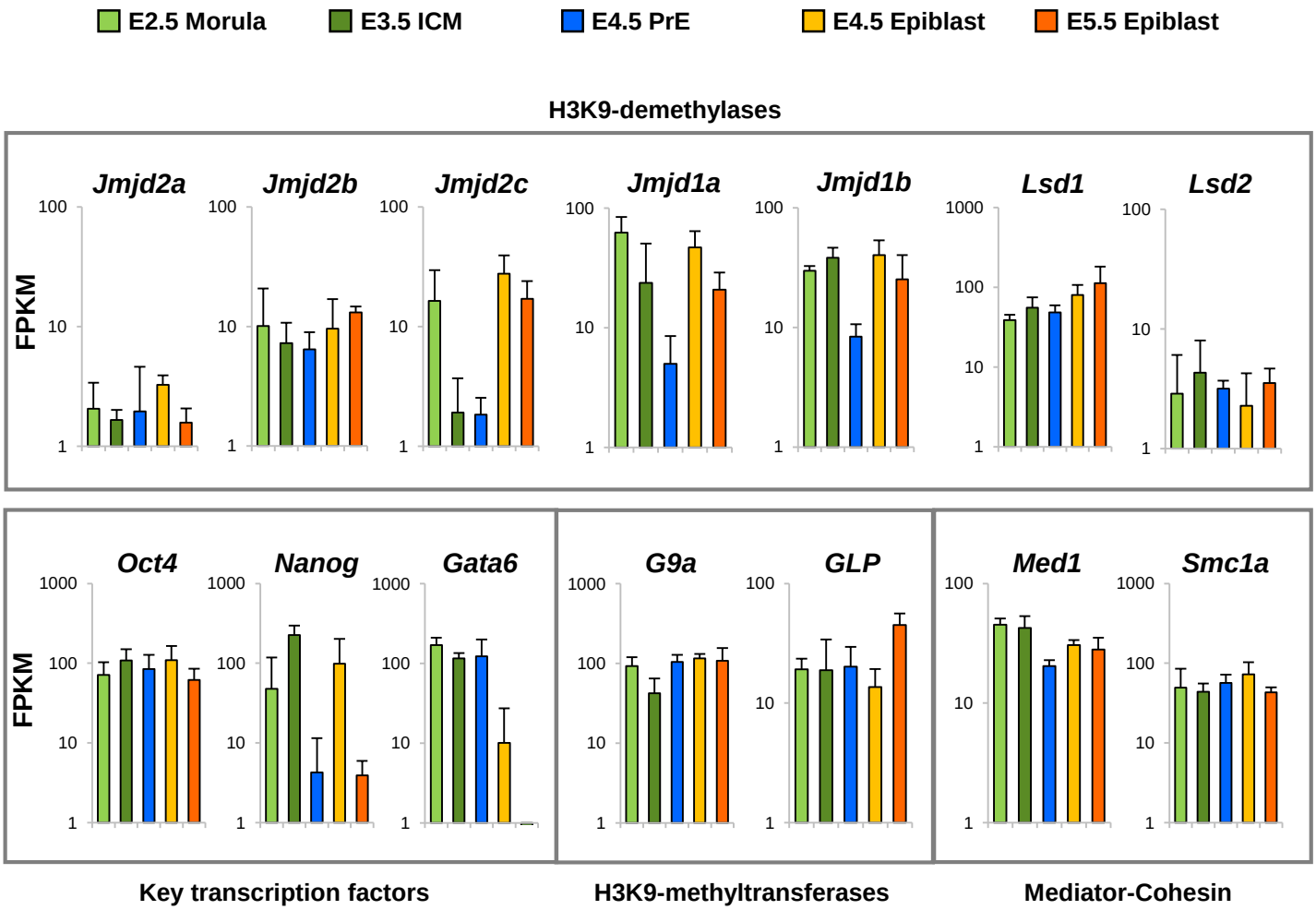

Fig. S3. *Jmjd2c* is dynamically expressed in the early mouse embryo. Comparative gene expression analysis at different developmental-times focussing on selected members of H3K9-demethylase families (*Jmjd2/Kdm4*: *Jmjd2a*, *Jmjd2b* and *Jmjd2c*; *Jmjd1/Kdm3*: *Jmjd1a* and *Jmjd1b*; *Kdm1*: *Lsd1* and *Lsd2*), epiblast (*Oct4* and *Nanog*) and primitive endoderm (*Gata6*) associated transcription factors, H3K9-methyltransferases (*G9a* and *GLP*) and the subunits of the Mediator (*Med1*) and Cohesin (*Smc1a*) complexes. Expression was assessed by RNA-seq in morula-stage embryos (E2.5), isolated inner cell mass (ICM) from early blastocysts (E3.5), dissected primitive endoderm (PrE) and epiblast layers from late blastocysts (E4.5) and in the post-implantation epiblast (E5.5), as previously published (Boroviak et al., 2015). Data are shown as the mean±s.d. of three independent pool samples in Fragments per Kilobase of Exon per Million Fragments (FPKM).

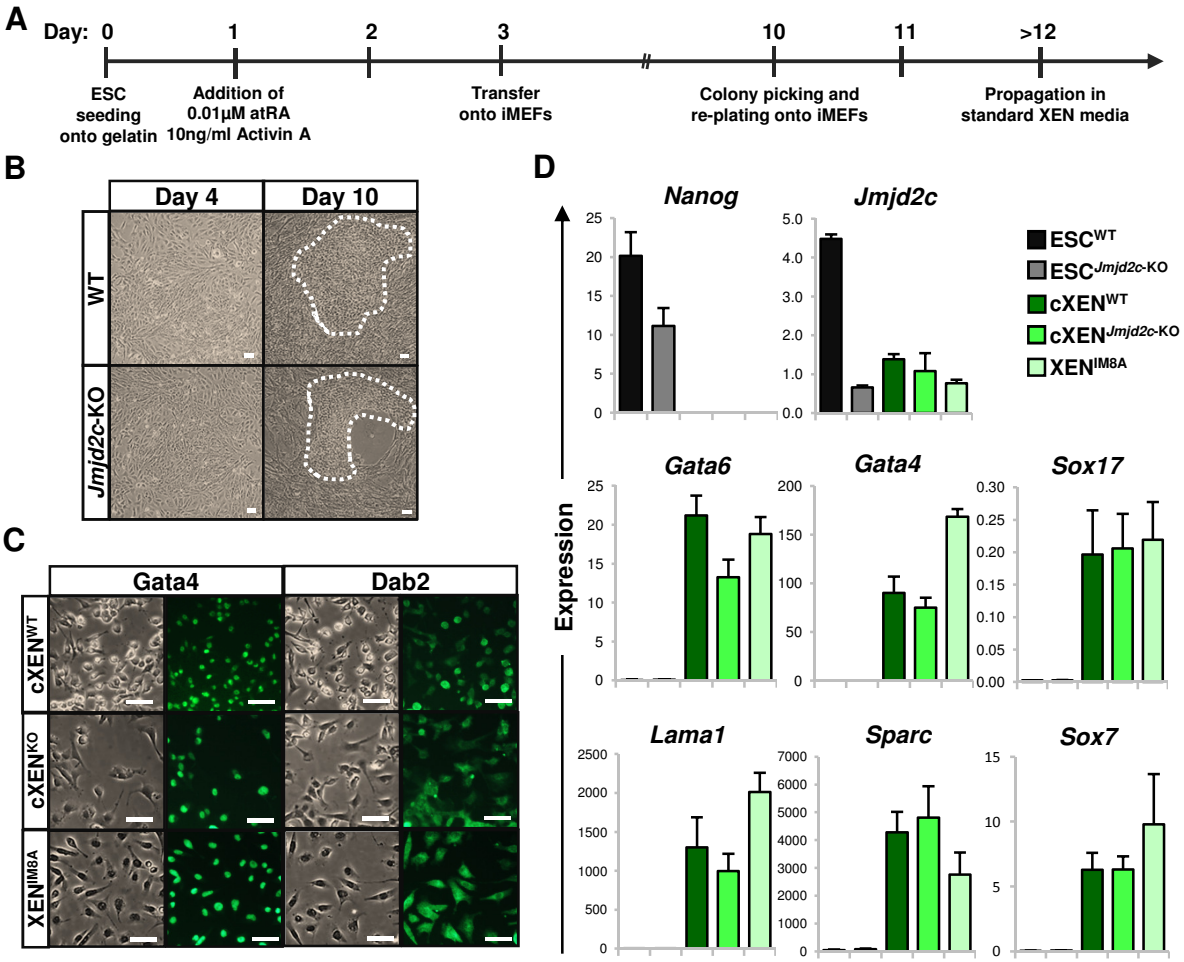

Fig. S4. *Jmjd2c*-knockout ESCs successfully generate self-renewing extra-embryonic endoderm (XEN) stem cells. (A-B) Timeline of ESC-to-XEN derivation protocol (adapted from Cho et al., 2012), and phase-contrast images of WT and *Jmjd2c*-KO ESC clone E3 cultures upon XEN cell conversion at the indicated time points. Bars, 100 µm. (C) Phase-contrast and staining for Gata4 and Dab2 of stably ESC-derived WT and *Jmjd2c*-KO converted XEN (cXEN) cells, and a control embryo-derived XEN cell line (IM8A). Bars, 100 µm. (D) Transcript levels of *Nanog*, *Jmjd2*c and XEN-associated markers (*Gata6*, *Gata4*, *Sox17*, *Lama1*, *Sparc* and *Sox7*) in WT and *Jmjd2c*-KO ESCs, cXEN cells, and embryo-derived XEN cells. Data were normalized to housekeeping genes, and expressed as the mean±s.e.m. of three biological replicates.

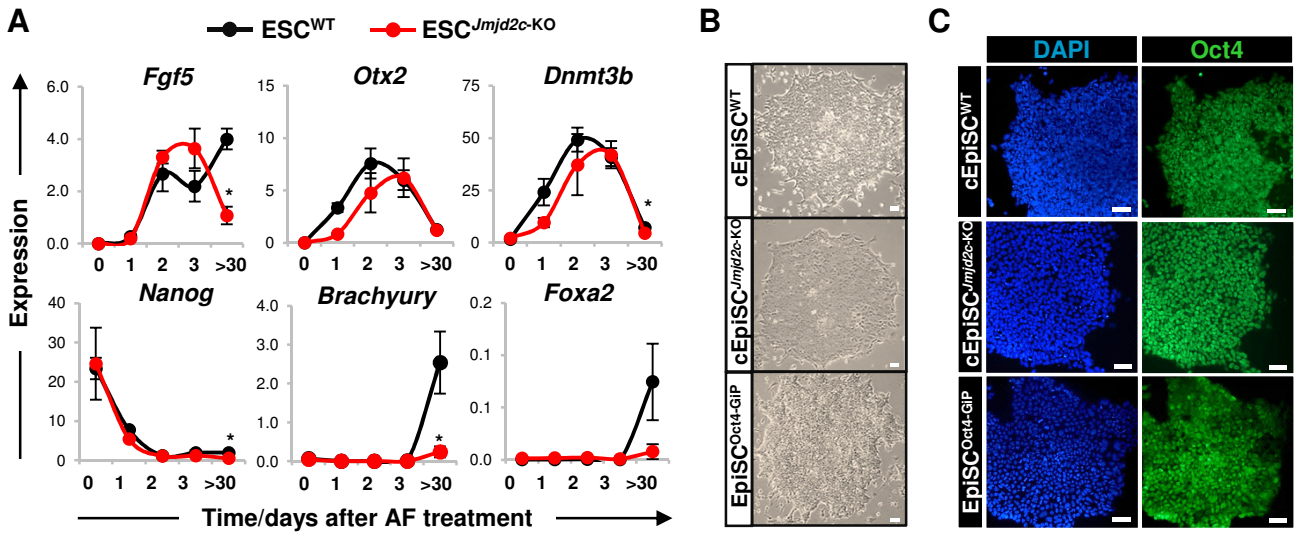

Fig. S5. *Jmjd2c*-knockout ESCs adopt an immature epiblast stem cell (EpiSC) phenotype. (A) Transcript levels of epiblast (*Fgf5*, *Otx2*, and *Dnmt3b*), pluripotency (*Nanog*) and differentiation (*Brachyury* and *Foxa2*) markers upon conversion of WT and *Jmjd2*-KO ESCs into EpiSCs (day 0 to 3) and in stably converted EpiSCs (cEpiSCs; day >30) in the presence of Activin and Fibroblast growth factor (AF). Data were normalized to housekeeping genes, and expressed as the mean±s.e.m. of at least three biological replicates. **P*<0.05; Mann-Whitney *U* test. (B) Phase-contrast images of stably derived cEpiSC cell lines from WT (cEpiSC^{WT}) and *Jmjd2c*-KO (cEpiSC$^{Jmjd2c\text{-}KO}$) clone E3 ESCs, and a control embryo-derived EpiSC line in which GFP expression is coupled with Oct4 (Oct4-GiP). Bars, 100 µm. (C) Oct4 labelling and DAPI staining in stable WT and *Jmjd2c*-KO cEpiSCs, and in control embryo-derived EpiSCs$^{Oct4\text{-}GiP}$. Bars, 100 µm.

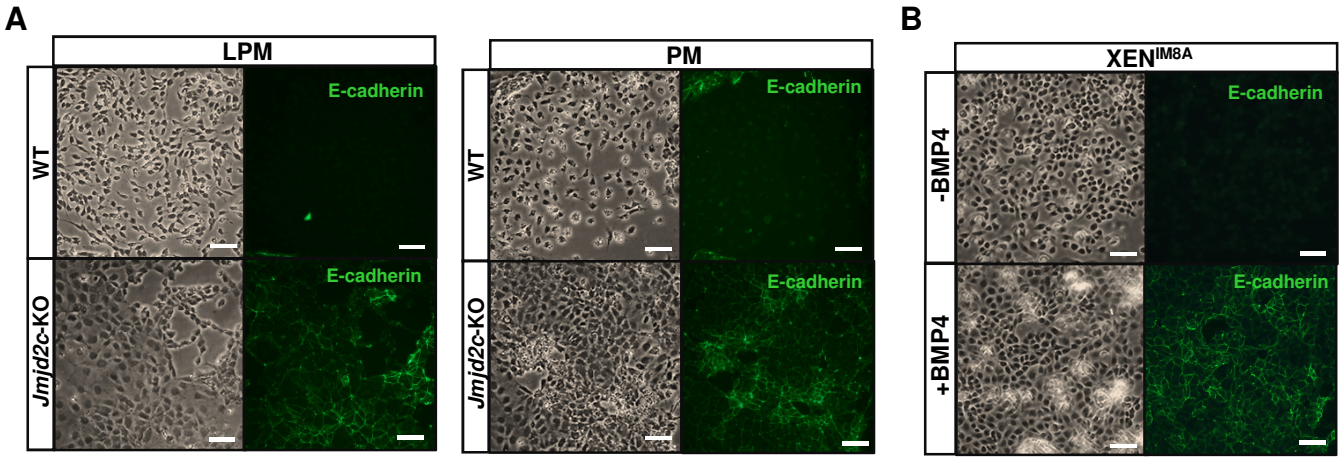

Fig. S6. Skewed differentiation into extra-embryonic endoderm (XEN)-like phenotype upon mesodermal induction of *Jmjd2c*-knockout cEpiSCs. Phase-contrast images and E-cadherin labelling of WT and *Jmjd2c*-KO cEpiSCs at day 4 of differentiation into lateral plate (LPM) and paraxial (PM) mesoderm cell types (A), and of XEN^{IM8A} cells with and without BMP4 treatment (B). Bars, 100 µm.

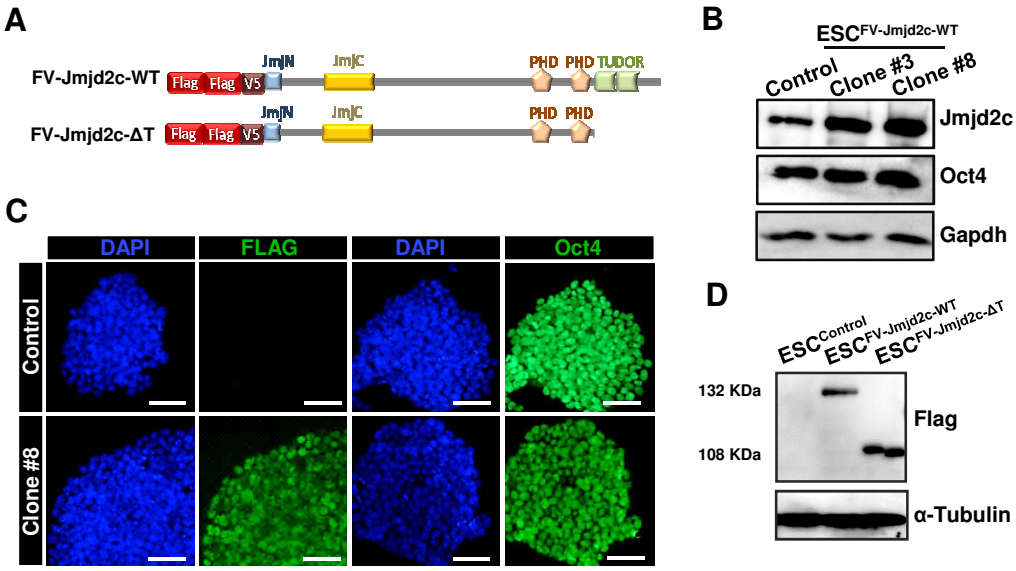

Fig. S7. Characterization of ESC clones stably expressing double-tagged wild-type and mutant Jmjd2c proteins. (A) Scheme of generated Flag(x2)-V5 tagged full-length wild-type (FV-Jmjd2c-WT) and mutated (FV-Jmjd2c-ΔT) Jmjd2c construct where both Tudor domains were deleted. Both constructs were used to generate stable ESC lines. An empty version of the same construct (without Jmjd2c) was used to generate a control ESC line. (B) Western blot of whole cell extracts of independent FV-Jmjd2c-WT (clone#3 and #8) and control ESC clones showing Jmjd2c and Oct4 protein levels. Gapdh was used as a loading control. (C) Labelling of the Flag epitope or Oct4 (green), and DAPI staining (blue) in control and FV-Jmjd2c-WT clone#8 ESCs. Bars, 100 µm. (D) Western blot showing protein levels of the Flag epitope in FV-Jmjd2c-WT clone#3 (132 KDa) and FV-Jmjd2c-ΔT clone#1 (108 KDa) ESC lines. α-Tubulin was used as a loading control.

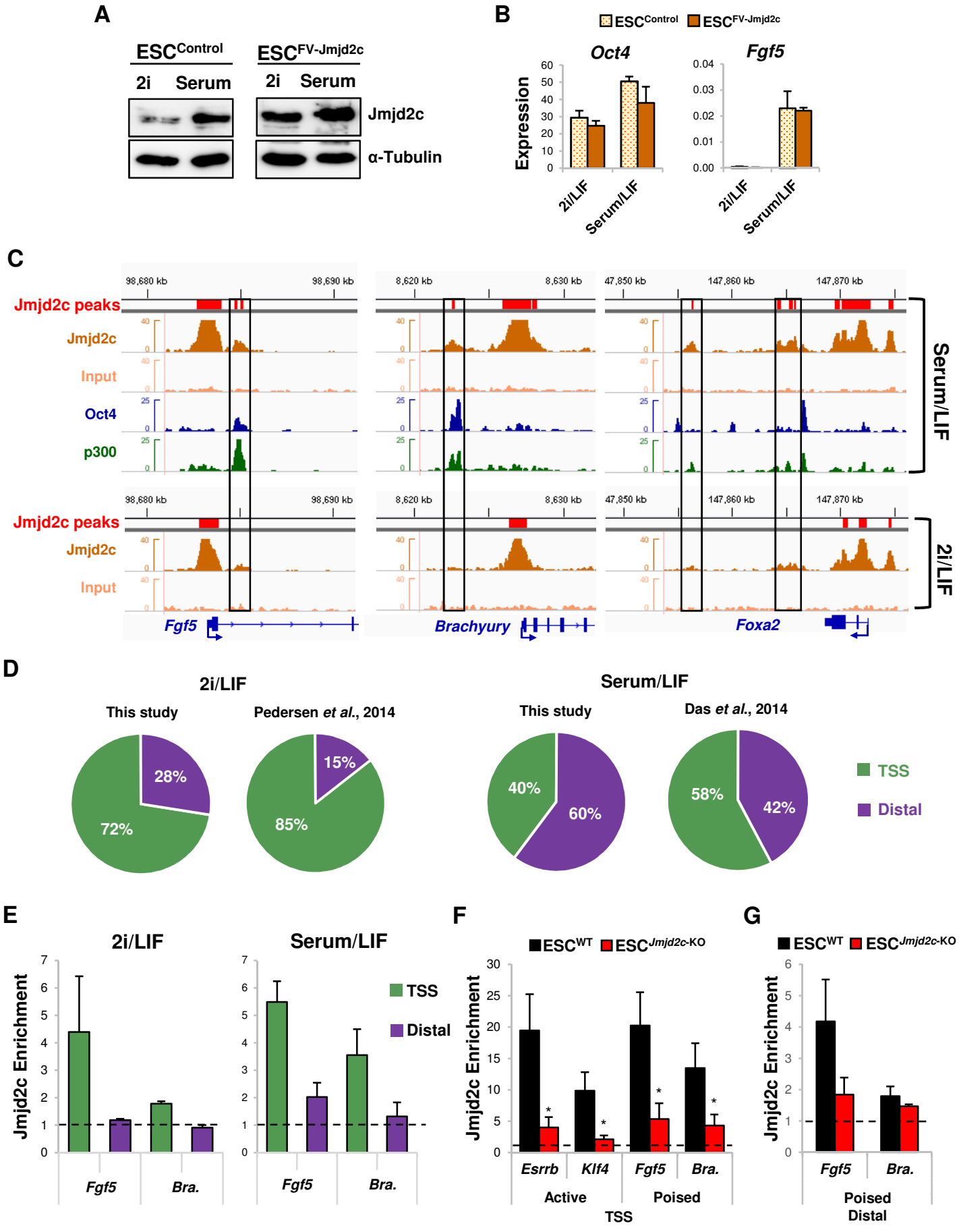

Fig. S8. Jmjd2c is re-distributed to lineage-specific enhancers during the priming of ESCs for differentiation. (A) Western blot showing Jmjd2c protein levels in control and FV-Jmjd2c-WT clone #8 ESCs cultured in either 2i/LIF or serum/LIF conditions. α-Tubulin was used as a loading control. (B) Expression of the pluripotency (*Oct4*) and early epiblast-associated (*Fgf5*) genes in control and FV-Jmjd2c-WT ESCs routinely cultured in 2i/LIF and serum/LIF showing the detection of *Fgf5* transcript in primed (serum/LIF) ESC cultures in contrast to naïve (2i/LIF) cells. Data were normalized to housekeeping genes, and expressed as the mean±s.e.m. of three biological replicates. (C) ChIP-seq binding profiles showing Jmjd2c peaks at the TSS regions of the lineage-specific *Fgf5*, *Brachyury* and *Foxa2* genes in 2i/LIF conditions (bottom panel), and the acquisition of additional Jmjd2c peaks overlapping with p300 and Oct4 at distal sites in the vicinity of the same genes in serum/LIF conditions (top panel). (D) Percentage of Jmjd2c-bound TSS (green) and distal (purple) peaks detected in primed (serum/LIF) and naïve (2i/LIF) conditions using datasets generated in this study and in previously published reports as indicated. (E) Enrichment levels for endogenous Jmjd2c binding at TSS and distal (enhancer) regions of *Fgf5* and *Brachyury* loci in formaldehyde-fixed chromatin from wild-type JM8-ESCs routinely cultured in 2i/LIF and serum/LIF conditions. Data were expressed as average fold enrichment over negative control region (intergenic; dotted line), and represent the mean±s.e.m. of three independent experiments. (F) Specificity of endogenous Jmjd2c ChIP was validated by assessing enrichment for Jmjd2c at active (*Esrrb* and *Klf4*) and poised (*Fgf5* and *Brachyury*) TSS regions extracted from wild-type (WT) JM8-ESCs and *Jmjd2c*-knockout (*Jmjd2c*-KO) ESCs. Data were expressed as average fold enrichment over negative control region (intergenic; dotted line), and represent the mean±s.e.m. of three independent experiments. (G) Enrichment levels of endogenous Jmjd2c binding at distal regions of *Fgf5* and *Brachyury* in WT versus *Jmjd2c*-KO ESCs. Data were expressed as average fold enrichment over negative control region (intergenic; dotted line), and represent the mean±s.e.m. of three independent experiments. **P*<0.05; Mann-Whitney *U* test.

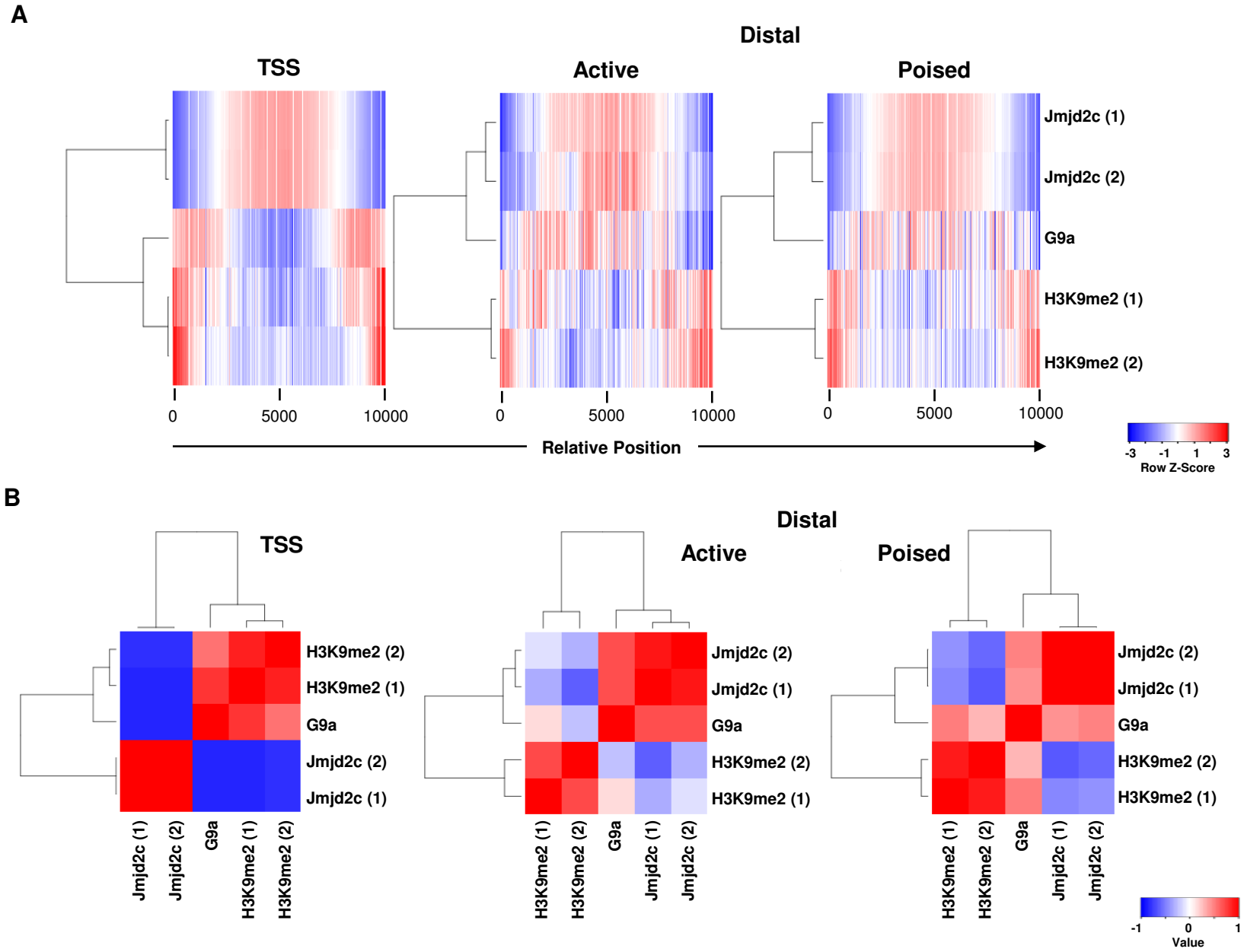
A
Distal
TSS
Active
Poised
Jmjd2c (1)
Jmjd2c (2)
G9a
H3K9me2 (1)
H3K9me2 (2)
0
5000
10000
Relative Position
-3
-1
1
3
Row Z-Score
B
Distal
TSS
Active
Poised
H3K9me2 (2)
H3K9me2 (1)
G9a
Jmjd2c (2)
Jmjd2c (1)
-1
0
1
Value

Fig. S9. G9a and Jmjd2c overlap genome-wide in ESCs at both active and poised enhancer regions in the absence of H3K9me2 deposition. (A) Heatmap representation of the distribution (i.e. binned mean ChIP-seq read density) of Jmjd2c (1: this study; 2: Das et al., 2014), G9a (Mozzetta et al., 2014), H3K9me2 (1: Liu et al., 2015; 2: Das et al., 2014) across Jmjd2c-bound TSS or active and poised distal sites. Each ChIP-seq experiment was adjusted for sequencing depth and normalised to their respective input. The colour key from blue to red indicates the enrichment levels from low to high, respectively. (B) Heatmap showing Pearson correlation between the distributions of Jmjd2c (1: this study; 2: Das et al., 2014), G9a (Mozzetta et al., 2014), H3K9me2 (1: Liu et al., 2015; 2: Das et al., 2014) across Jmjd2c-bound TSS or active and poised distal sites. The colour key from blue to red indicates the correlation coefficient from low to high, respectively.

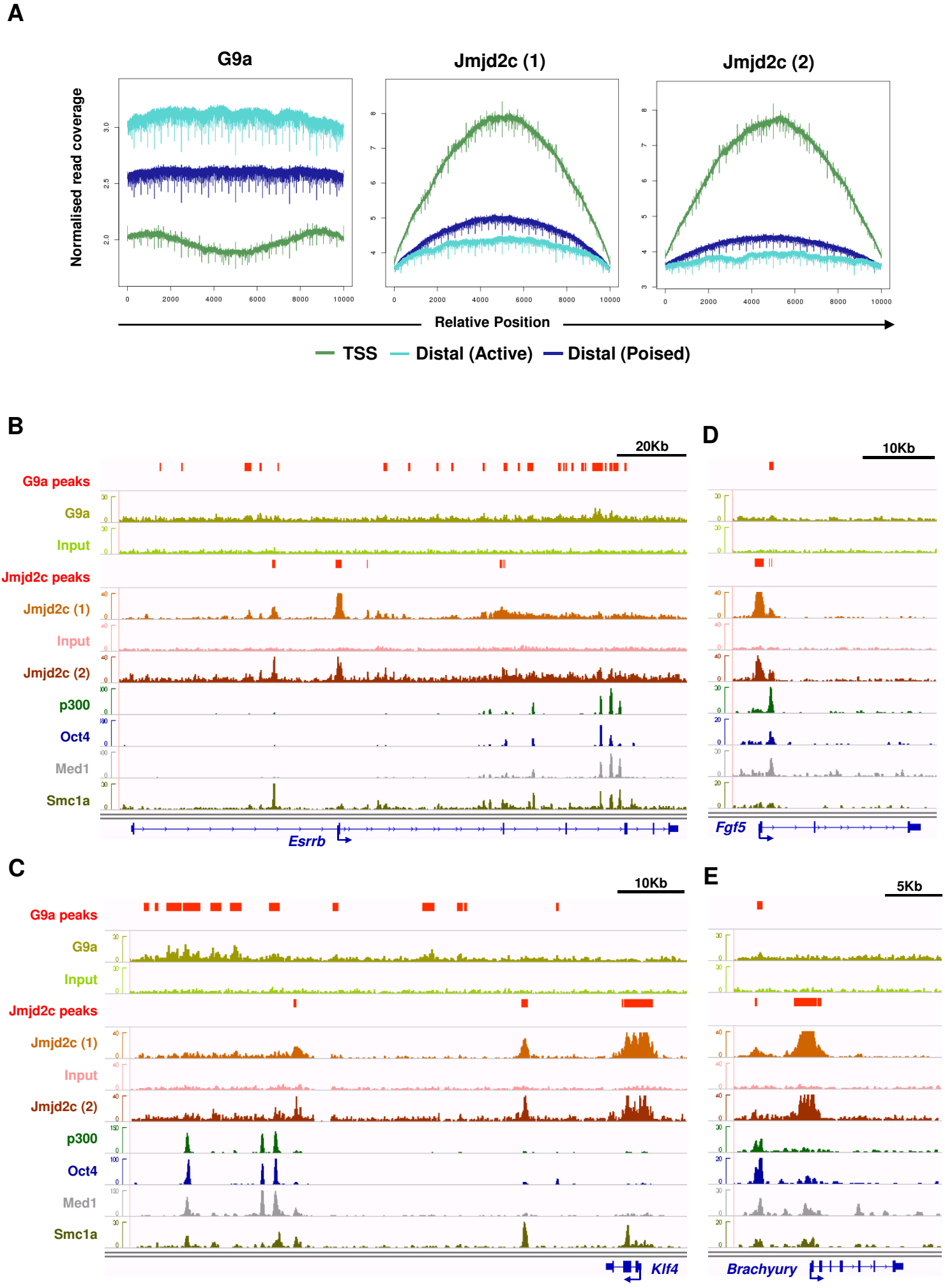

Fig. S10. G9a highest density binding is observed at Jmjd2c-bound active enhancer regions in ESCs. (A) Coverage plot representation of the distribution (i.e. binned mean ChIP-seq read density) of G9a (Mozzetta et al., 2014) and Jmjd2c (1: this study; 2: Das et al., 2014) at Jmjd2c-bound TSS (green), distal active (light blue) and distal poised (dark blue) sites. Each ChIP-seq experiment was adjusted for sequencing depth and normalised to their respective input. (B) ChIP-seq binding profiles for G9a (Mozzetta et al., 2014) and Jmjd2c (1: this study; 2: Das et al., 2014), alongside with published profiles for the enhancer-associated factors p300, Oct4, Med1 and Smc1a, at the active enhancer regions of *Esrrb* (B) and *Klf4* (C) loci, and the poised enhancers of *Fgf5* (D) and *Brachyury* (D) loci. Red bars represent peaks called relative to respective input control samples for G9a (Mozzetta et al., 2014) and Jmjd2c (this study) ChIP-seq datasets.

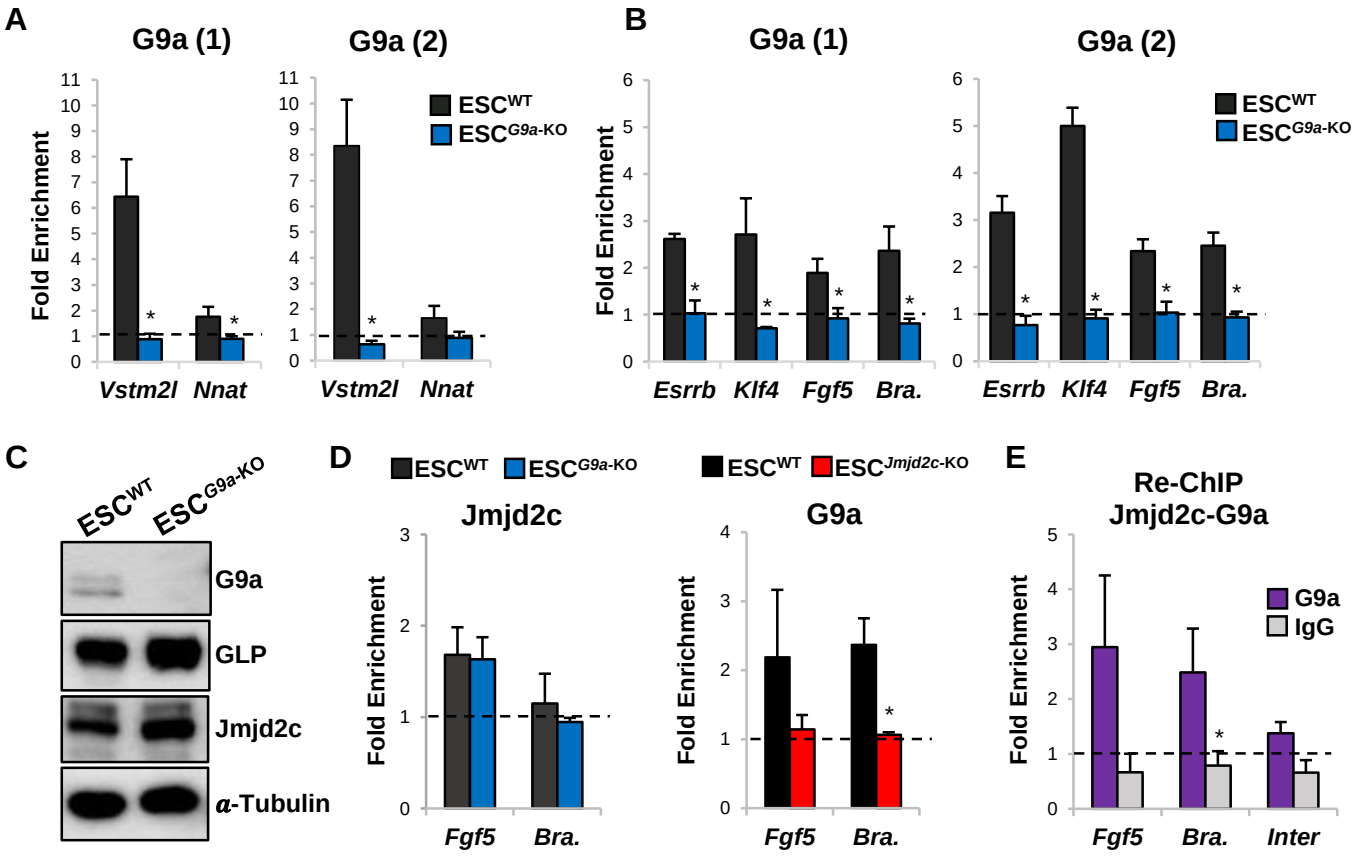

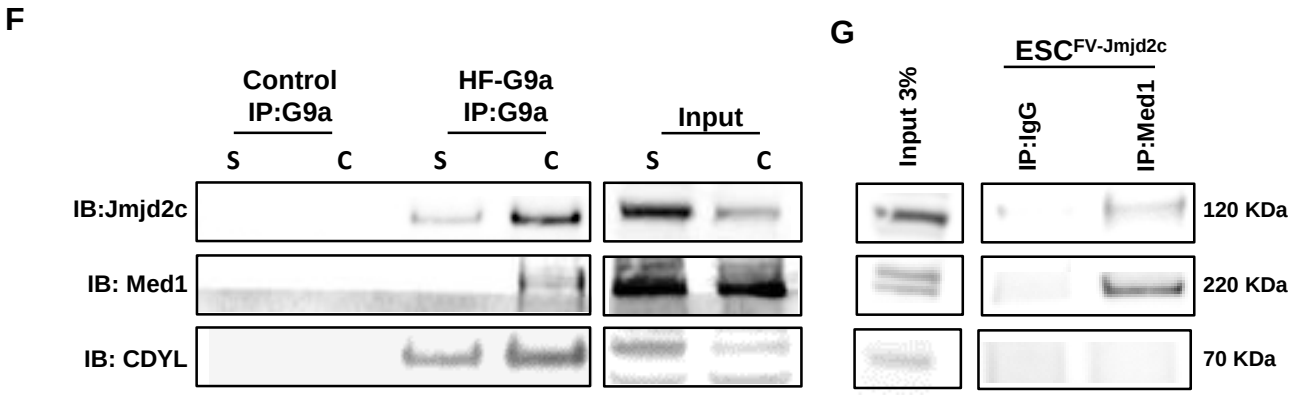

Fig. S11. Jmjd2c facilitates G9a binding at lineage-specific enhancers in ESCs. (A) Specificity of two anti-G9a antibodies (1: Cell Signalling; 2: R&D) was validated in ChIP-qPCR by assessing enrichment levels for G9a at previously reported regions with high (*Vstm2l*) and low (*Nnat*) enrichment in wild-type (WT) TT2-ESCs and *G9a*-knockout (*G9a*-KO) in serum/LIF conditions. Data were expressed as average fold enrichment over negative control region (intergenic; dotted line), and represent the mean±s.e.m. of three independent experiments. **P*<0.05; Mann-Whitney *U* test. (B) Specificity of anti-G9a antibodies (1: Cell Signalling; 2: R&D) was also validated in ChIP-qPCR by assessing enrichment levels for G9a at the enhancer regions of active (*Esrrb* and *Klf4*) and transcriptionally primed (*Fgf5* and *Brachyury*) genes in WT and *G9a*-KO ESCs in serum/LIF conditions. Data were expressed as average fold enrichment over negative control region (intergenic; dotted line), and represent the mean±s.e.m. of three independent experiments. **P*<0.05; Mann-Whitney *U* test. (C) Western blot using anti-G9a, anti-GLP and anti-Jmjd2c antibodies of whole cell extracts from WT and *G9a*-KO ESCs. α-Tubulin was used as a loading control. (D) Enrichment levels for endogenous Jmjd2c at *Fgf5* and *Brachyury* enhancer regions in WT and *G9a*-KO ESCs (left panel). Enrichment levels for G9a at *Fgf5* and *Brachyury* enhancer regions in wild-type (WT) JM8-ESCs and *Jmjd2c*-knockout (*Jmjd2c*-KO) (right panel). Data were expressed as average fold enrichment over negative control region (intergenic; dotted line), and represent the mean±s.e.m. of three independent experiments. (E) Co-binding of Jmjd2c and G9a was validated at *Fgf5* and *Brachyury* enhancer regions by sequential ChIP (Re-ChIP) in ESCs expressing Flag-tagged Jmjd2c. Jmjd2c was immunoprecipitated using anti-Flag antibodies, followed by immunoprecipitation with anti-G9a (R&D), IgG or beads only. An intergenic region was included to confirm background levels. Data were expressed as fold enrichment over beads only control (dotted line), and represent the mean±s.e.m. of three independent experiments. **P*<0.05; Mann-Whitney *U* test. (F) G9a interaction partners were purified with a double immunoprecipitation (IP) with anti-Flag and anti-HA antibodies in soluble (S) and chromatin (C) nuclear fractions of HeLa cells expressing an empty vector (Control) or tagged (HF-G9a) G9a protein. (G) Med1 immunoprecipitation was performed in nuclear fractions of ESCs expressing a Flag-tagged Jmjd2c (FV-Jmjd2c). Interactions were visualised by immunoblotting (IB) with anti-Med1, anti-Jmjd2c or anti-CDYL antibodies. Data are representative of duplicate experiments. The input and IgG lanes of Jmjd2c correspond to the same experiment as Figure 5D.

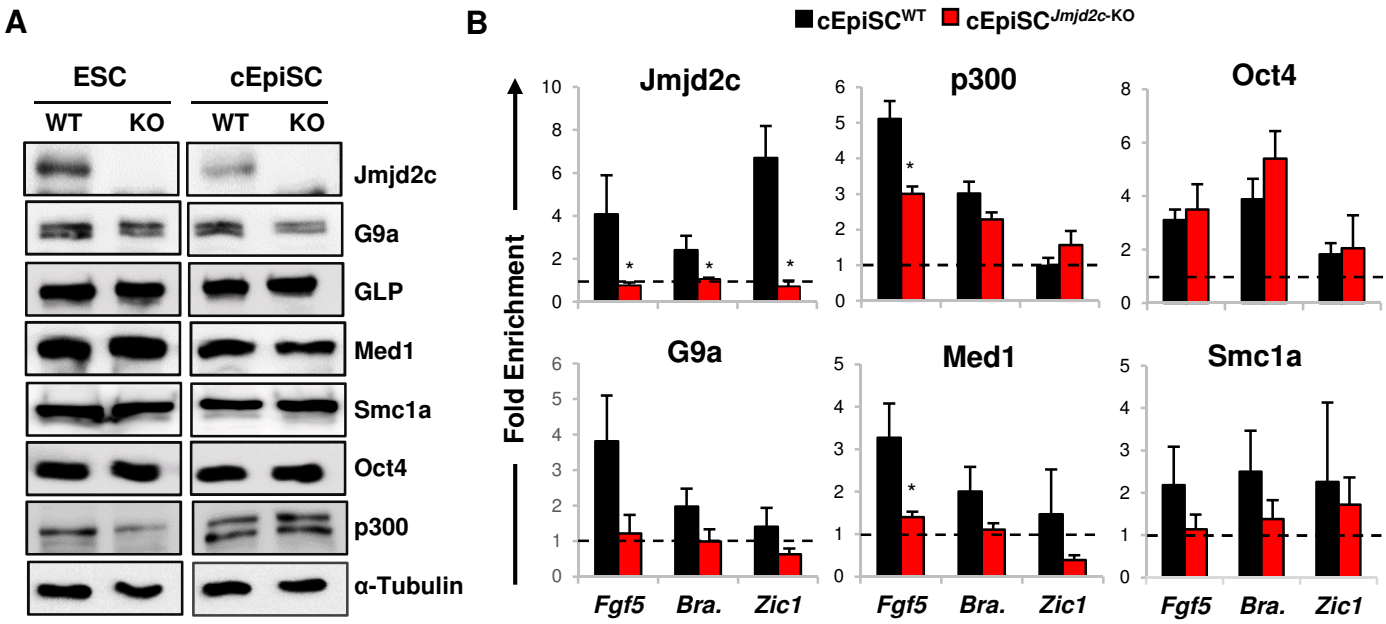

Fig. S12. Loss of Jmjd2c compromises G9a, Med1 and Smc1a binding at Oct4-bound poised enhancers in ESC-derived cEpiSCs. (A) Western blot using antibodies against Jmjd2c, G9a, GLP, Med1, Smc1a, Oct4 and p300 in whole cell extracts from wild-type (WT) JM8-ESCs, *Jmjd2c*-knockout (*Jmjd2c*-KO) ESCs and derived cEpiSCs. α-Tubulin was used as a loading control. (B) Enrichment levels for Jmjd2c, p300, Oct4, G9a, Med1 and Smc1a at the active *Fgf5* (PE) and poised *Brachyury* and *Zic1* enhancers as assessed by ChIP-qPCR in WT and *Jmjd2c*-KO cEpiSCs. Data were expressed as average fold enrichment over negative control region (intergenic; dotted line), and represent the mean±s.e.m. of three independent experiments. **P*<0.05; Mann-Whitney *U* test.

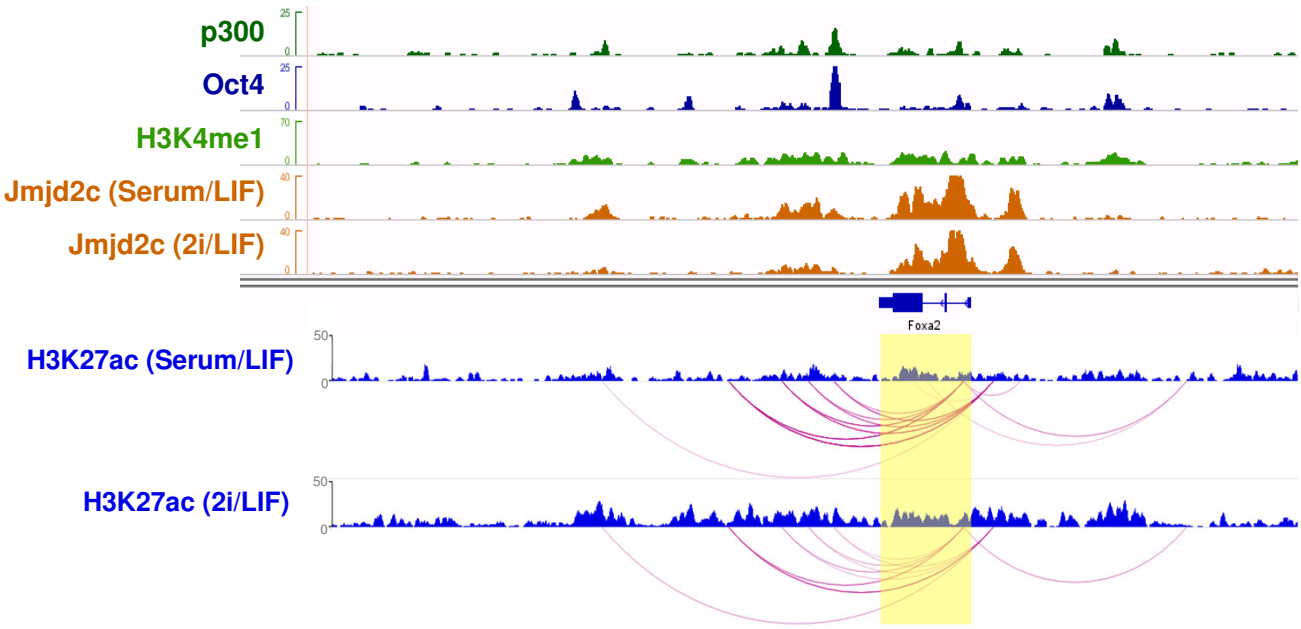

Fig. S13. Chromatin dynamics across *Foxa2* locus in naïve (2i/LIF) and primed (serum/LIF) ESCs. ChIP-seq binding profiles showing p300, Oct4, H3K4me1 and Jmjd2c in either serum/LIF or 2i/LIF conditions across the *Foxa2* locus (top panel). Interaction profile for the promoter of *Foxa2* visualized for ESCs grown in either serum/LIF or 2i/LIF conditions (bottom panel). Pink arcs represent interactions from *Foxa2* promoter identified using CHiCAGO pipeline (Cairns et al., 2015) based on newly generated high coverage capture Hi-C datasets (O. Joshi, H.G. Stunnenberg, unpublished). The depth of pink colour of each interaction arc represents the strength of the interaction.

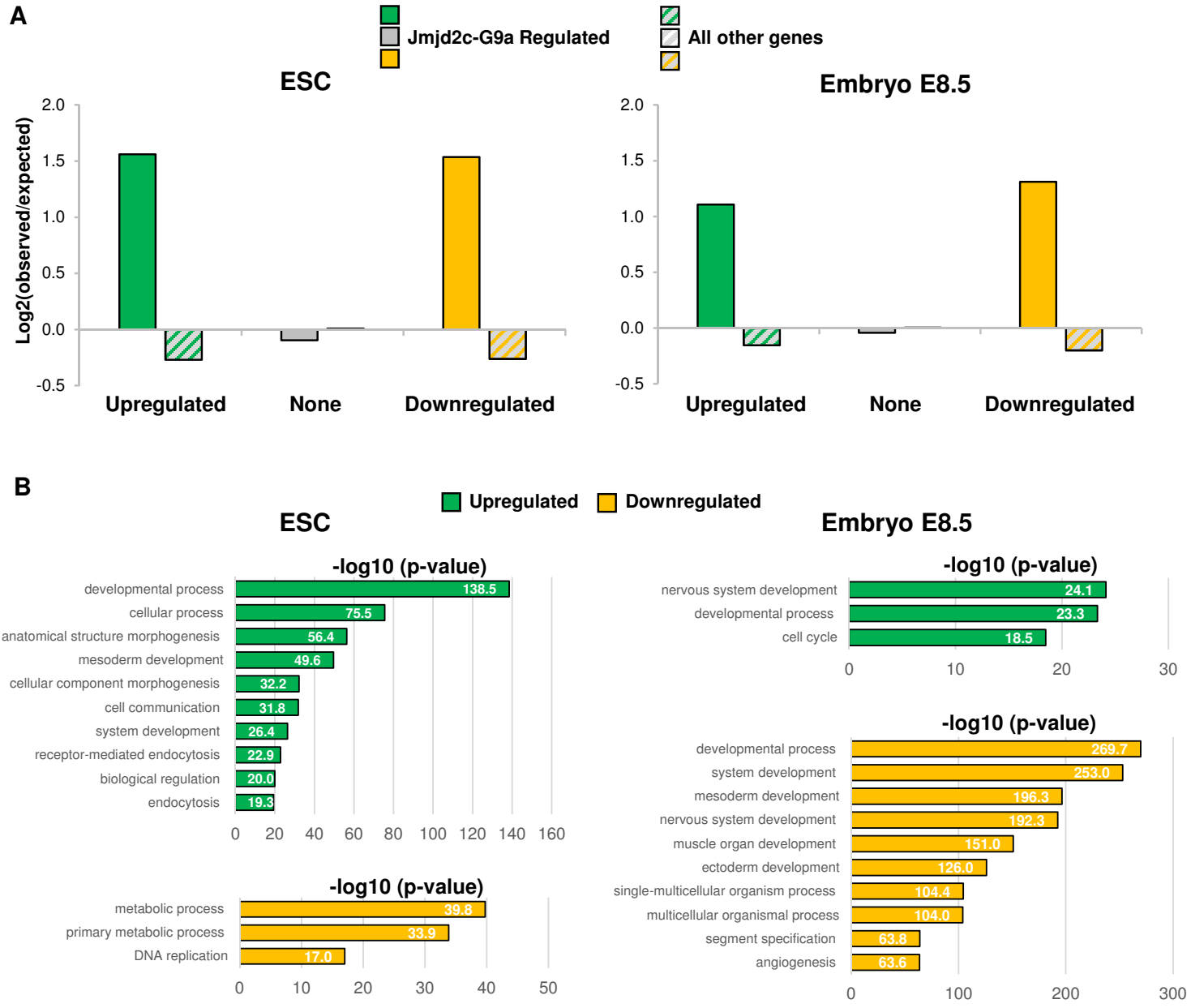

Fig. S14. Jmjd2c-G9a co-bound developmental genes are downregulated in the embryo in the absence of *G9a*. (A) Enrichment of Jmjd2c-G9a regulated genes amongst genes differentially expressed in *G9a*-knockout ESCs and embryos at E8.5. Upregulated (log2 fold-change >0, *q-value* <0.05) and downregulated (log2 fold-change <0, *q-value* <0.05) genes were defined from publicly available RNA-seq datasets profiling gene expression in ESCs (GSE) and E8.5 embryos (GSE) with and without *G9a* knockout (Auclair et al., 2016; Mozzetta et al., 2014). Expected numbers in each set were calculated from the proportions of all measured genes belonging to each category (upregulated, downregulated, and none). Difference of observed numbers from expected were evaluated with Chi-squared test giving *P*-value = 3.10E-93 and 1.00E-83 in ESC and E8.5 embryo samples, respectively. (B) Top 10 most significant biological processes of Jmjd2c-G9a regulated genes that are either up (green) or downregulated (yellow) in *G9a*-knockout ESCs (left panel) or *G9a*-knockout embryos at E8.5 (right panel).

Table S1. Antibodies used in this study

Primary Antibody	Catalogue Number	Supplier	Concentration/Quantity		
			Western Blot	IF	ChIP
Cdyl	ab5188	Abcam	1:1000	-	-
Dab2	sc13982	SantaCruz	-	1:250	-
E-Cadherin	U3254	Sigma-Aldrich	-	1:500	-
Flag M2	F1804	Sigma-aldrich	1:1000	1:500	10 µg
G9a	3306	Cell Signalling	1:1000	-	0.24 µg
G9a	PP-A8620A-00	R&D	-	-	5 µg
Gata4	sc-9053	SantaCruz	-	1:250	-
Gata6	AF1700	R&D Systems	-	1:500	-
GFP	ab290	Abcam	-	1:1000	-
GLP	PP-B0422-00	R&D Systems	1:1000	-	-
H3	ab1791	Abcam	1:50,000	-	-
H3K27ac	ab4729	Abcam	-	-	5 µg
H3K27me3	07-449	Millipore	1:100,000	-	-
H3K36me3	mAb-183-050	Diagenode	1:10,000	-	-
H3K4me2	07-030	Millipore	1:50,000	-	-
H3K9me2	ab1220	Abcam	1:20,000	-	2 µg
H3K9me3	ab8898	Abcam	1:100,000	-	-
Jmjd2b	A301-478A	Bethyl Laboratories	1:2000	-	-
Jmjd2c	-	H.H. Ng's lab	1:2000	-	-
Jmjd2c	sc-104949	SantaCruz	1:1000	-	5 µg
Med1	A300-793A	Bethyl Laboratories	1:1000	-	8 µg
Oct4	sc-8628	SantaCruz	1:1000	-	5 µg
Oct4	sc-5279	SantaCruz	-	1:200	-
p300	sc-585	SantaCruz	1:1000	-	5 µg
Phalloidin	P1951	Sigma-Aldrich	-	1:100	-
Smc1a	A300-055A	Bethyl Laboratories	1:1000	-	8 µg
α-Tubulin	T6074	Sigma-Aldrich	1:20,000	-	-

Table S2. Sequences of primers used for genotyping

Name	Sequence (5' – 3')	Allele
tm1a-F	GAAGTAGGAGGAGAACCATAGTTCCAGAG	First
tm1a-R	GCCTCTTCGCTATTACGCCAGCTG	
tm2-F	AAGAGGTAAGAAGCCCATCACATC	Second
tm2-R	GCAGCTATTTACCCGCAGGA	

Table S3. Sequences of primers used for cloning of Jmjd2c

Name	Sequence (5' – 3')	Vector
XhoI-Jmjd2c-F	ATACATTCTCGAGATGGAGGTGGT	pPy-CAG-Jmjd2c
PacI-Jmjd2c3-R	CTCTTAATTAACTACTGTCTCTTCTGACACT	
BamHI-Jmjd2c-F	ATTAGGATCCGAGGTGGTGGAGGTG	FV-Jmjd2c-WT
SalI-Jmjd2c-R	TAATGTCGACCTACTGTCTCTTCTGACACTT	
SalI-Del-Tudor-R	TAATGTCGACCTACGCGTTTGAGTTGAC	FV-Jmjd2c-ΔT

Table S4. Sequences of primers used for RT-qPCR

Gene	Forward (5' – 3')	Reverse (5' – 3')
Oct4	CGTGGAGACTTTGCAGCCTG	GCTTGGAAACTGTTCTAGCTCCT
Brachyury	CCGGTGCTGAAGGTAAATGT	CCTCCATTGAGCTTGTTGGT
*Brachyury**	TCAGCAAAGTCAAACTCACC	TCATTCTGGTAGGCAGTCAC
Cxcr4	CGGGATGAAAACGTCCATTT	ATGACCAGGATCACCAATCCA
Dnmt3b	TTCAGTGACCAGTCCTCAGACACGAA	TCAGAAGGCTGGAGACCTCCCTCTT
Setb1	GAGGCCGGGGAGAGGCTGAA	TAGCTGGTCGGCGAAGCCCT
Esrrb	GCACCTGGGCTCTAGTTGC	TACAGTCCTCGTAGCTCTTGC
Fgf5	TGTGTCTCAGGGGATTGTAGG	AGCTGTTTTCTTGGAATCTCTC
*Fgf5**	ACGTTTTCTTCGTCTTCTGC	TTCCTACAATCCCCTGAGAC
Flk-1	GACGGAGAAGGAGTCTGTGC	TTTCTGTGTGCTGAGCTTGG
Foxa2	CCATCAGCCCCACAAAATG	CCAAGCTGCCTGGCATG
*Foxa2**	ACTGGAGCAGCTACTACGC	AGGATGACATGTTCATGGAG
G9a	TCACCCTGACTGACAATGAG	AGACAGGAACAACAGAACAC
Gapdh	AGAAGGTGGTGAAGCAGGCA	CGAAGGTGGAAGAGTGGGAG
Gata4	GAACACCCTGAGCAGGCCTC	TTTCTGGGAAACTGGAGCTGG
Gata6	GAGCTGGTGCTACCAAGAGG	TGCAAAAGCCCATCTCTTCT
GLP	CAGATGGAGAAACAAATGGGTCT	TTTGCTTCCCCACTTCTGTGT
Hmbs	ACTGGTGGAGTATGGAGTCTAGATGGC	GCCAGGCTGATGCCCAGGTT
Isl1	AGACCCTCTCAGTCCCTTG	CGTCATCTCCACTAGTTGCTC
Jmjd1a	GAGCCACAGTCGGAGACTTC	TTGGCCATCAGATCATCAAA
Jmjd2a	TTCTGTGAATCCTGCGTCTG	TAGCTGTGCACGGTGAGAAC
Jmjd2b	CATGTGGAAGACCACGTTTG	AAGGGGATGCCGTACTTCTT
Jmjd2c	GATGACTGGCCTTACGTGGT	CTTCACACAGTTTCGGCTCA
Klf4	GTGCCCCGACTAACCGTTG	GTCGTTGAACTCCTCGGTCT
L19	TGATCTGCTGACGGAGTTG	GGAAAAGAAGGTCTGGTTGGA
Lrp2	CCTTGCCAAACCCTCTGAAAAT	CACAAGGTTTGCGGTGTCTTTA
Lsd1	GATGATGTCTGGGAAACAGG	GGGCCAAGGTAGAATACAGAG
Math1	*GGAGAAGCTTCGTTGCACGC*	*GGGACATCGCACTGCAATGG*
Meox1	ACGGAGAAGAAATCATCCAG	GTAGTTGTGGTGGGCAAAC
Mixl1	GACAGACCATGTACCCAGAC	GCTTCAAACACCTAGCTTCAG
Nanog	CTTACAAGGGTCTGCTACTGA	TCTGCTTCCTGGCAAGGACC
Otx2	TATCTAAAGCAACCGCCTTACG	AAGTCCATACCCGAAGTGGTC
Pax3	GGGAACTGGAGGCATGTTTA	GTTTTCCGTCCCAGCAATTA
Pdgfrα	GGTCCCAACCTGTAATGAAG	GTAAATGGGACCTGACTTGG
S17	ATGACTTCCACACCAACAAGC	GCCAACTGTAGGCTGAGTGAC
Sox17	GGAATCCAACCAGCCCACTG	GGACACCACGGAGGAAATGG
Sox7	CAAGGATGAGAGGAAACGTCTG	TCATCCACATAGGGTCTCTTCTG
Sparc	AGGGCCTGGATCTTCTTTCTC	CAAATTCTCCCATTTCCACCT
Suv39h1	TGTCAACCATAGTTGTGATCC	ATTCGGGTACTCTCCATGTC
Suv39h2	ATCTACGAATGCAACTCAAGGTG	CCACAGCCATTGCTAGTTCTAA
Tbx3	GAACCTACCTGTTCCCGGAAA	CAATGCCCAATGTCTCGAAAAC
Ywhaz	CGTTGTAGGAGCCCGTAGGTCAT	TCTGGTTGCGAAGCATTGGG

** Primers used in Figure2.*

Table S5. Sequences of primers used for ChIP-qPCR

Gene	Forward (5' – 3')	Reverse (5' – 3')	Region
Intergenic	AAGGGGCCTCTGCTTAAAA	AGAGCTCCATGGCAGGTAGA	Control
Vstm2l	GCACGGCTCACAGTACCTAAAGT	CAGCAAGCACGGTGTGTCA	5' TSS
Nnat	CCCTACCCAACCCATCCTATC	CCACCGCGGCACTTTG	Gene body
Esrrb	CTCCCACTCCGCCTTCTC	GGCAAATCACGCGGAAGA	TSS
	GGAAGTGGGAAGTGTTGCTAT	GAGCTCCAGATCCCCTACAC	Enhancer
Klf4	AAGGAAGGCGTTCCAGATTT	TTGAGATCCCTGGTGAAAGG	TSS
	CGCCTGCCTGTACCTTCTAA	GGGCCTGGGAGAGATTGTAA	Enhancer
Fgf5	CTCACCAGTCGCAGCTTCT	GAAGGGCTCCACTGGAAACT	TSS
	GTGCATGCATGGGACTGTAG	AACCCGACCTGAACCTAGTG	Enhancer
	TTGGACTGCTGGGGATAGTG	CACGGGGTAAGGTGCTTCTA	Enhancer 1
	GGGGCTTGGAGAGTTCAGAT	AAAGCTCACCTGGCAGTCTA	Enhancer 3
Brachyury	GGCCGACTTTGTTTCTTCCC	GAATGCCTCCTTCCTCCTCA	TSS
	CTCTGTCTCAGTTTGCCATTCTC	TGTACCGACCACTGGAATCC	Enhancer
Zic1	CCCAGTCACAGGAACAGGATA	GGCCGCCACTACAAGAATT	Enhancer

Table S6. Sequences of primers used for H3K9me2 ChIP-qPCR

Gene	Forward (5' – 3')	Reverse (5' – 3')	Region
Brachyury	GGATTCCAGTGGTCGGTACA	AGGCTCTTGGCTCCAGCTAGT	Enhancer
	ACCAAGAACGGCAGGTAGGT	GCTGTTAACTCAGCGGGAAG	TSS
	CAAGCCTCCCTGCTGACTT	GGTTCAGCCACTGACACTCA	Control
Fgf5	GCCGACCAGTCTCTTTCATT	TTGCTTCTCCTTCTGCACCT	Enhancer
	GGCTCGGAACATAGCAGTTT	GCCCAAAGGAATCTTGACC	TSS
	GTGTCCCATGGTAACCTGCT	GCAGCCCTGTACAAGATCCA	Control
Magea2	TTGGTGGACAGGGAAGCTAGGGGA	CGCTCCAGAACAAAATGGCGCAGA	TSS

Supplementary Materials and Methods

Generation and rescue of *Jmjd2c*-knockout ESCs

Wild-type JM8-ESC lines from the C57BL/6N mouse background and a mutant ESC line carrying one *Jmjd2c* targeted null allele were obtained from the EUCOMM/IKMC repository (Bradley et al., 2012; Skarnes et al., 2011). The knockout first allele (tm1a) was generated by gene targeting through replacement mutagenesis with a gene-trapping cassette encoding lacZ/β-galactosidase and a neomycin resistance gene, upstream of a "critical exon" common to all predicted *Jmjd2c* transcripts (Fig. S1A). The generation of biallelic gene targeted cell lines was then carried out through insertional mutagenesis, introducing a second gene-trap cassette through homologous recombination into the second allele (tm2) of *Jmjd2c*, encoding the hygromycin resistance gene and GFP (Fig. S1A) (C. Fisher and W. C. Skarnes, in

preparation). Both cassettes are promoterless, hence relying on the active transcription of *Jmjd2c*, and contain an En2 splice acceptor (SA) signal and the SV40 polyadenylation (pA) sequences to ensure transcripts are spliced into the cassette and stopped at the inserted sites, which is predicted to lead to nonsense mediated decay of these transcripts. FRT sites in the first allele allow the removal of the cassette with FLP recombinase, whereas the loxP sites inserted in the vicinity of the critical exon allow the generation of a conditional null allele with Cre recombinase, however neither of these strategies was used in this study. Validation of the correct insertion of the targeting cassettes was achieved by long-range PCR using the Expand Long Template PCR kit (Roche) with the primers listed in Table S2. Two *Jmjd2c*-knockout clones E2 and E3 were selected for further studies, showing a complete loss of Jmjd2c protein expression as assessed by western blotting. The wild-type (WT) and the two *Jmjd2c*-knockout (*Jmjd2c*-KO) embryonic stem cell clones (E2 and E3) derived from the same parental line were routinely cultured in Knockout-DMEM media (Gibco) supplemented with batch tested 10% fetal bovine serum (FBS), β-mercaptoethanol, L-glutamine, penicillin-streptomycin and LIF (made in house). G418 (100 µg/mL) and Hygromycin B (25 µg/mL) were routinely added to the culture medium in the *Jmjd2c*-KO cell lines for selection and removed prior to any experiment.

For rescue of the expression of *Jmjd2c*, the full-length transcript was amplified from the cDNA of WT ESCs and ligated into a pPyCAG-Ires-Puro vector (primer sequences in Table S3). Approximately 3 x 10^5 *Jmjd2c*-KO clone E3 ESCs were transfected with Lipofectamine 2000 (Invitrogen) and 2 µg of pPyCAG-Jmjd2c (Rescue) or an empty pPyCAG vectors (Control), then 1 µg/mL Puromycin (Sigma-Aldrich) was added for selection 24 hours post-transfection. After 8 days of selection individual ESC clones were isolated and expanded.

Generation of *Jmjd2c*-knockdown ESCs

Approximately 10^5 E14Tg2A (E14) ESCs were transfected with Lipofectamine 2000 and 1 µg of either of two independent shRNA vectors generated against *Jmjd2c* or a control vector as described in Loh et al., 2007. 24 hours post-transfection 1 µg/mL Puromycin was added for selection and cells harvested after 96 hours of Puromycin selection for subsequent analysis. For generation of stable *Jmjd2c*-knockdown ESC lines, cells were treated 24 hours post-transfection with Puromycin for 8-10 days, colonies picked individually and expanded in GMEM (Gibco) supplemented with 10%

FBS, β-mercaptoethanol, L-glutamine, sodium bicarbonate, sodium pyruvate, non-essential amino acids, penicillin-streptomycin, LIF and Puromycin.

Generation of FV-Jmjd2c ESCs

The full-length *Jmjd2c* transcript was amplified from WT ESCs cDNA and ligated into a pPyCAG-Ires-Puro vector containing a Flag-Flag-V5 at the N-terminal side (primer sequences in Table S3). Approximately 10^6 E14-ESCs were transfected with Lipofectamine 2000 and 4 µg of Flag-Flag-V5-Jmjd2c (FV-Jmjd2c) or an empty vector (Control). 24 hours post-transfection 1 µg/mL Puromycin was added for selection and after 8-10 days of culture individual ESC clones were isolated and expanded indefinitely under selection. Cell lines were maintained in GMEM (Gibco) supplemented with 10% FBS, β-mercaptoethanol, L-glutamine, sodium bicarbonate, sodium pyruvate, non-essential amino acids, penicillin-streptomycin, LIF and Puromycin.

Self-renewal assay

To assess the self-renewal ability of ESC populations, 100/cm^2 cells were seeded in duplicate in serum-containing medium supplemented with LIF. After 5 days the colonies were stained for alkaline phosphatase (AP) activity (Sigma-Aldrich) following the manufacturer's recommendations. Colony morphology was scored as differentiated (<20% stained), mixed (>20%-90% stained), undifferentiated (>90% stained).

Differentiation of ESCs

For induction of embryoid bodies (EBs), 10^5/cm^2 cells were cultured in suspension in ultra-low attachment plates (Corning) in ESC media (see Supplemental Materials and Methods) supplemented with 5% FBS without LIF. For all-trans retinoic-acid (atRA) induced differentiation, 2 x 10^5/cm^2 cells were seeded in ESC media for 24 hours. Media was then changed into ESC media supplemented with 5% FBS, and 1 µM of atRA without LIF. EB aggregates and atRA treated cells were collected at the indicated time points for expression analysis, and at day 4 for immunofluorescence staining (atRA assay).

Conversion of ESCs into XEN cells

Conversion of ESCs into XEN cells was performed as described in Niakan et al., 2013. Briefly, 3,000/cm^2 cells were plated in ESC media. After 24 hours the media was replaced with XEN derivation media: Advanced RPMI (Gibco) with 15% FBS (Biosera), β-mercaptoethanol and penicillin-streptomycin, freshly supplemented with

10 ng/mL Activin A (R&D), 0.01 µM all-trans retinoic acid (Sigma-Aldrich), 24 ng/mL bFgf (Peprotech) and 1 µg/mL Heparin (Sigma-Aldrich). After 48 hours of derivation cells were re-plated onto a layer of irradiated MEFs, and maintained in media supplemented with bFgf and Heparin for approximately 10 days. Converted XEN (cXEN) colonies were then manually picked and expanded on 0.1% gelatin coated plates in standard XEN media: Advanced RPMI with 15% FBS, β-mercaptoethanol and penicillin-streptomycin. Embryo-derived XEN^{IM8A} cells (Kunath et al., 2005) were cultured in the same conditions.

Conversion of ESCs into EpiSCs

Conversion of ESCs into EpiSCs was performed as described in Guo et al., 2009. Briefly, ESCs were firstly adapted into serum-free culture conditions in N2B27 (Gibco) medium supplemented with 1 µM PD0325901 (Mek inhibitor), 3 µM CHIR99021 (Gsk3 inhibitor) and LIF (in house) for 7 days prior to conversion (Ying et al., 2008). Approximately 5,000/cm^2 cells were plated in 2i/LIF media on fibronectin-coated plates. After 24 hours the media was changed into N2B27 supplemented with 20 ng/mL Activin A (in house) and 12 ng/mL bFgf (epiblast media). After 10-12 days converted EpiSC (cEpiSC) colonies were detached following incubation with PBS, and expanded in epiblast media in plates coated with 10% FBS. Embryo derived EpiSCs$^{Oct4\text{-}GiP}$ (Guo et al., 2009) were cultured in the same conditions.

Mesoderm induction

Converted EpiSCs and embryo-derived EpiSCs were cultured in N2B27 (Guo et al., 2009) or chemically defined media with BSA (CDM-BSA) (Brons et al., 2007), respectively, both supplemented 20 ng/mL Activin A (in house) and 12 ng/mL Fibroblast growth factor (bFgf) (Petrotech). Colonies were dissociated by incubation in PBS and seeded in their respective media at a ratio of 1:6 to 1:10 in plates previously coated with 0.1% gelatin followed by MEF medium (Advanced DMEM/F-12 supplemented with 10% FBS). After 24 hours the media was changed into FLyB media consisting of CDM-PVA supplemented with 20 ng/µl bFgf, 10 nM LY294002 (Sigma) and 10 ng/mL BMP4 (R&D). Following 36 hours of mesoderm induction in FLyB conditions, the media was changed into either FB40 – 20 ng/µl bFgf and 40 ng/mL BMP4, or FLyWLDN – 20 ng/ul bFgf, 2 nM LY294002, 2 ng/mL Wnt3a (Peprotech) and 250 nM LDN193189 (Sigma-Aldrich), for lateral plate mesoderm and paraxial mesoderm differentiation, respectively. Differentiated EpiSCs were

harvested at the indicated time points for expression analysis, and at day 4 for flow cytometry analysis and immunofluorescence staining.

Immunoblotting analysis

Cell lysis was carried out using RIPA buffer (50 mM Tris, 1 mM EDTA, 0.5 mM EGTA, 1% Triton X-100, 0.1% sodium deoxycholate and 140 mM NaCl) supplemented with proteinase and phosphatase inhibitors (Roche). Histones were acid extracted as previously described (Shechter et al., 2007). Protein concentrations of whole cell extracts and acid-extracted histones were measured using a Bradford assay (Thermo Fisher Scientific). The appropriate amounts of whole cell lysates (10-50 µg) or histones (2 µg) were resolved on an 8% or 13% SDS-PAGE gel, respectively, and subsequently transferred into methanol-activated polyvinylidene fluoride membranes (GE Healthcare). Membranes were blocked with 5% skimmed milk (Sigma) for 1 hour and incubated with the appropriate antibodies (see Table S1).

Quantitative PCR

Total RNA was isolated and DNaseI-treated using the RNeasy mini kit (Qiagen). Samples were reverse-transcribed using SuperScript II (Invitrogen) following the manufacturer's instructions. For quantification, cDNA or DNA samples were amplified with Jumpstart SYBR Green PCR Mastermix or KicQstart SYBR Green PCR Mastermix (Sigma), and primer pairs listed in Supplemental Tables S4-S6, using a StepOne™ System (Applied Biosystems). For mesoderm induction RNA extraction was performed with TRIzol (Life Technologies) and samples were reverse transcribed using a QuantiTect Reverse Transcription kit (Qiagen) according to the manufacturer's directions. cDNA was amplified with a QuantiTect SYBR Green PCR kit (Qiagen) and primer pairs listed in Supplemental Table S4, using a Rotor Gene 6000 PCR system (Corbett Life Science).

Immunofluorescence staining

Cells were seeded on gelatinized glass coverslips or 12-well culture plates previously coated with 0.1% gelatin for 10 minutes followed by Advanced DMEM/F-12 with 10% FBS overnight. Cells were fixed in PBS with 4% paraformaldehyde (PFA) for 10 minutes and then permeabilized and blocked at room temperature for 30 minutes using 0.4% Triton X-100 in blocking buffer (10% serum and 90% PBS). Incubation with primary antibody (see Supplemental Table S1) was performed overnight at 4°C, and subsequently incubation with fluorophore-conjugated

secondary antibodies (ThermoFisher) diluted 1:500 for 1 hour at room temperature. Glass coverslips were mounted on Vectashield with DAPI (Vector Laboratories) and visualised using a SP5 Leica laser-scanning confocal microscope or an inverted fluorescent/brightfield microscope.

Flow cytometry analysis

Cells were harvested using cell dissociation buffer (Gibco) and 10^4 cells were blocked in PBS containing 2% FBS, stained for Flk-1 (5 µg/mL anti-Flk-1-Biotin, avas12 a1 clone, eBioscience, followed by 0.4 µg/mL APC-conjugated streptavidin, Biolegend) or Pdgfrα (2 µg/mL anti-Pdgfrα-PE, clone APA5, eBioscience) and analysed on an Accuri C6 Flow cytometer.

Co-immunoprecipitation

Immunoprecipitation of HA-Flag-G9a (HF-G9a) in fractionated nuclear extracts from HeLa cells was performed as previously described in Fritsch et al., 2010. Briefly, HeLa cell lines expressing a HA-Flag-G9a were generated, together with control cell line expressing an empty vector. Cells were lysed in a hypotonic buffer and disrupted with a Dounce homogenizer, and the cytosolic fraction was separated from nuclei (pellet) by centrifugation. The nuclear soluble and chromatin fractions were separated upon incubation in a high salt buffer followed by centrifugation. The chromatin fraction was further digested with micrococcal nuclease (Sigma-Aldrich). G9a-bound complexes were affinity purified by incubation with anti-Flag antibody bound beads (cat# A2220, Sigma-Aldrich). Complexes were eluted with a Flag peptide (Ansynth) and further purified on anti-HA antibody-conjugated agarose beads (cat# A2095, Sigma-Aldrich) and subsequently eluted with the HA peptide (Ansynth). Co-IPs in nuclear extracts of ESCs were performed as previously described (Battisti et al., 2016). Briefly, cells were lysed similarly as above and nuclei pellets were resuspended in sucrose buffer (20 mM Tris pH 7.65, 60 mM NaCl, 15 mM KCl; 0.34 M Sucrose) followed by an incubation in a high salt buffer (20 mM Tris-HCl pH 7.65, 0.2 mM EDTA, 25% glycerol, 900 mM NaCl, 1.5 mM $MgCl_2$) resulting in a final NaCl concentration of 300 mM. Nuclear extracts were digested with micrococcal nuclease and sonicated for 10 min (15 sec ON, 45 sec OFF) at high frequency. After pre-clearing, immunoprecipitations were performed overnight at 4°C with the corresponding amount of each antibody or IgG control. Complexes were purified with ultralink beads (Perbio), washed in wash buffer (50 mM Tris-HCl, pH 7.65, 150 mM NaCl, Triton X-100 0.5%) and eluted in NuPAGE® LDS Sample Buffer

(Life Technologies) at 96 °C during 5 min. Immunopurified complexes were resolved on 4-12% SDS-PAGE bis Tris acrylamide gradient gel and immunoblotted with the indicated antibodies (Table S1).

Chromatin immunoprecipitation

In general, chromatin immunoprecipitation (ChIP) of Flag, Jmjd2c, G9a, Med1, Smc1a, Oct4, p300 and H3K27ac followed the procedure described in (Frank et al., 2001), and for H3K9me2 the procedure described in Mozzetta et al., 2014, with the modifications outlined below. Unless stated otherwise, for Jmjd2c, Smc1a, G9a, H3K9me2 ChIPs and Flag-G9a re-ChIPs, cells were fixed with 2 mM Di-Succinimidyl Glutarate (SantaCruz) for 45 minutes at room temperature (Nowak et al., 2005), in addition to an initial 10 minutes fixation step with 1% Formaldehyde (Sigma-Aldrich). Chromatin samples were sonicated on a bioruptor (Diagenode) to produce fragments of 100-500 bp, and ChIPs performed with the antibodies listed in Table S1 and with ProteinG-coupled magnetic Dynabeads (Invitrogen). The amounts of chromatin (DNA or protein) used in each ChIP were as follows: 20 µg of DNA (H3K9me2), 250 µg (G9a), 400 µg (Oct4), 500 µg (Flag, Jmjd2c, p300, H3K27ac) and 800 µg (Med1, Smc1a) of protein. Following washes of bound DNA-protein complexes in the appropriate wash buffers in each referenced protocol, DNA was eluted in 1% SDS at 65°C and treated with 40 ng/µl RNaseA following 0.2 µg/µl Proteinase K. After phenol/chloroform purification, DNA was then precipitated at -20°C with 20-30 µg GlycoBlue carrier (Invitrogen), 1/10 volumes of 3 M NaAc and 2 volumes of 100% ethanol. Resuspended pellets were used for qPCR or for generation of libraries for sequencing. For sequential ChIP (re-ChIP), Flag-bound complexes were eluted at 37 °C for 30 minutes in 75µl of 1% SDS, supplemented with 15mM DTT (Bertero et al., 2015). The eluate was diluted 10 times in the same buffer used for IP and incubated at 4 °C for 5 h, before proceeding to the second round of immunoprecipitations with the G9a antibody, mouse IgG or no antibody (‘beads only’). The ‘beads only’ control was included to normalise for any background from the Flag antibody.

ChIP-sequencing and computational analysis

For sequencing of Flag-Jmjd2c bound DNA fragments, sequencing libraries were prepared using the NEBNext® Ultra™ DNA Library Prep Kit and Multiplex Oligos (New England Biolabs) from 5 ng of DNA. Following analysis on an Agilent Bioanalyzer libraries were pooled and sequenced on an Illumina Genome Analyzer II (Illumina). Quality of the sequenced reads was assessed using the FASTQC

program (Babraham Bioinformatics). Reads were aligned to the UCSC mouse reference genome (mm9) using Bowtie2 (Langmead and Salzberg, 2012), and only uniquely aligned reads were retained. Aligned reads (SAM) were converted into BED format to subsequently generate bigwig files for visualization in the IGV browser (Robinson et al., 2011). For each condition (2i/LIF and serum/LIF), the input and two biological duplicates were sequenced. Due to the high correlation between bigwig files of each pair of replicates, individual BAM files were merged and used in peak calling. List of enriched peaks were obtained using MACS2 with an FDR <0.0001 by calling peaks relative to the respective input control samples (background). Gene annotation to the nearest TSS and motif enrichment analysis was performed using HOMER (Heinz et al., 2010), respectively. For the charts in Figure S8D, the same treatment was applied to the ChIP-seq profiles referenced. Density plots and heatmaps in Figure 3C,E and Figure 5A were generated with deepTools (Ramirez et al., 2014). Overlaps between two genomic intervals were identified with the Intersect function in usegalaxy.org (Blankenberg et al., 2010; Giardine et al., 2005; Goecks et al., 2010). Counts for generation of Venn Diagrams in Figure 5B between three datasets were obtained using the R package ChiPpeakAnno (Zhu et al., 2010). To identify the functional classification listed on Figure 3G, Jmjd2c-bound H3K27-low genomic regions were inputted into GREAT (Genomic Regions Enrichment of Annotations Tool) and tested against the mouse genome (McLean et al., 2010).

For the analysis in Figure 4, S9 and S10 ChIP-seq data were downloaded from Genome Expression Omnibus (GEO) as SRA files, converted to FASTQ format using fastq-dump.2.4.2, evaluated using FASTQC program (Babraham Bioinformatics), trimmed and filtered using Trimmomatic-0.33 (LEADING:10 TRAILING:10 SLIDINGWINDOW:4:18 MINLEN:20) (Bolger et al., 2014). Sequences were aligned to the mm9 version of the mouse genome using Bowtie2. To calculate the average ChIP-seq read coverage at Jmjd2c-bound sites, BAM files were read into R, duplicate reads were removed and the bam files were converted to coverage objects using the Genomic Alignments package (Lawrence et al., 2013). The coverage objects were normalised to both sequencing depth and their respective inputs as follows:

$$F = 10^6/T$$
$$N_S = CF$$
$$N = \frac{N_S}{I}$$

Where T is the total number of reads, F is the sequencing depth normalisation factor, C is the pre-normalised read coverage, N_S is the sequencing depth normalised read coverage, I is the input read coverage and N is the sequence read and input normalised read coverage.

Coverage heatmaps were generated using the gplots package (Zhang, 2016). To plot the coverage heatmaps values greater than 3 standard deviations from the mean were removed and replaced values imputed by the mice R package. The largest number of values replaced from a single dataset was 69 out of 10,000 (0.7%). Pearson correlation coefficients of the average read coverage were calculated and visualised as heatmaps.

The accession numbers of the published ChIP-seq datasets analysed are listed below. Raw or treated files were obtained directly from the GEO repository, the mouse ESC ChIP-seq compendium (Martello et al., 2012) or the Supplementary Information of the referenced paper. For G9a, bigwig files were generated using the parameters described in Mozzetta et al., 2014.

Accession	Reference	Factor	BED files	BigWig files
GSE11724	Marson et al., 2008	Oct4	Kagey et al., 2010	Compendium
GSE22562	Kagey et al., 2010	Med1	Kagey et al., 2010	Compendium
GSE22562	Kagey et al., 2010	Smc1a	Kagey et al., 2010	Compendium
GSE24165	Creyghton et al., 2010	p300	Creyghton et al., 2010	Compendium
GSE46536	Mozzetta et al., 2014	G9a	GEO	Generated
GSE43229	Das et al., 2014	Jmjd2c	Generated	Generated
GSE53936	Pedersen et al., 2014	Jmjd2c	Generated	Generated
GSE48519	Hon et al., 2014	H3K4me1	-	GEO
GSE48519	Hon et al., 2014	H3K27ac	-	GEO
GSE48519	Hon et al., 2014	H3K4me3	-	GEO
GSE27827	Lienert et al., 2010	H3K4me2	-	GEO
GSE54412	Liu et al., 2015	H3K9me2	-	Generated
GSE43229	Das et al., 2014	H3K9me2	-	Generated

RNA-seq analysis

RNA-seq was treated as described above and were aligned to the mm9 version of the mouse genome using tophat-2.1.0 (Trapnell et al., 2009). Transcript assembly and differential expression analysis was performed using the cufflinks-2.2.1 suite of

software (Trapnell et al., 2013; Trapnell et al., 2010). TopHat aligned reads were assembled using Cufflinks, the final transcriptome assembly was generated using Cuffmerge and differential expression was evaluated using Cuffdiff. Chi-square tests were performed on the Cuffdiff evaluated differentially expressed gene lists. The genes were divided into Jmjd2c-G9a regulated and all other annotated genes. Up and downregulated genes were defined as those with statistically significant (*q-value* <0.05) log2 fold-changes in expression between the *G9a*-knockout and wild-type cells. Non-differentially expressed genes were defined as those with a non-significant change in expression (*q-value* >0.05). The functional classification of both sets of genes was identified through a statistical enrichment test using default settings in PantherDB GO (Mi et al., 2013).

Capture Hi-C in ESCs

To identify integration profile for promoter of *Foxa2* in Figure S13, the CHiCAGO pipeline was used to output scores for capture Hi-C data from the study Joshi et al., 2015. A manuscript on the CHiCAGO pipeline (Cairns et al., 2016) is publically available, with the pipeline itself at regulatorygenomicsgroup.org/chicago. Probe targeted Dpn2 fragments from *Foxa2* gene promoter were used as regions of interest and interactions anchored at the same region, with a threshold CHiCAGO score of 5 were considered. For further information on capture Hi-C or interaction calling and scoring please refer to (Joshi et al., 2015) and (Cairns et al., 2016).

Supplementary References

Battisti, V., Pontis, J., Boyarchuk, E., Fritsch, L., Robin, P., Ait-Si-Ali, S. and Joliot, V. (2016). Unexpected Distinct Roles of the Related Histone H3 Lysine 9 Methyltransferases G9a and G9a-Like Protein in Myoblasts. *J Mol Biol* **428**, 2329-2343.

Bertero, A., Madrigal, P., Galli, A., Hubner, N. C., Moreno, I., Burks, D., Brown, S., Pedersen, R. A., Gaffney, D., Mendjan, S., et al. (2015). Activin/nodal signaling and NANOG orchestrate human embryonic stem cell fate decisions by controlling the H3K4me3 chromatin mark. *Genes Dev* **29**, 702-717.

Blankenberg, D., Von Kuster, G., Coraor, N., Ananda, G., Lazarus, R., Mangan, M., Nekrutenko, A. and Taylor, J. (2010). Galaxy: a web-based genome analysis tool for experimentalists. *Curr Protoc Mol Biol* **Chapter 19**, Unit 19 10 11-21.

Bolger, A. M., Lohse, M. and Usadel, B. (2014). Trimmomatic: a flexible trimmer for Illumina sequence data. *Bioinformatics* **30**, 2114-2120.

Brons, I. G., Smithers, L. E., Trotter, M. W., Rugg-Gunn, P., Sun, B., Chuva de Sousa Lopes, S. M., Howlett, S. K., Clarkson, A., Ahrlund-Richter, L., Pedersen, R. A., et al. (2007). Derivation of pluripotent epiblast stem cells from mammalian embryos. *Nature* **448**, 191-195.

Cairns, J., Freire-Pritchett, P., Wingett, S. W., Varnai, C., Dimond, A., Plagnol, V., Zerbino, D., Schoenfelder, S., Javierre, B. M., Osborne, C., et al. (2016). CHiCAGO: robust detection of DNA looping interactions in Capture Hi-C data. *Genome Biol* **17**, 127.

Frank, S. R., Schroeder, M., Fernandez, P., Taubert, S. and Amati, B. (2001). Binding of c-Myc to chromatin mediates mitogen-induced acetylation of histone H4 and gene activation. *Genes Dev* **15**, 2069-2082.

Giardine, B., Riemer, C., Hardison, R. C., Burhans, R., Elnitski, L., Shah, P., Zhang, Y., Blankenberg, D., Albert, I., Taylor, J., et al. (2005). Galaxy: a platform for interactive large-scale genome analysis. *Genome Res* **15**, 1451-1455.

Goecks, J., Nekrutenko, A., Taylor, J. and Galaxy, T. (2010). Galaxy: a comprehensive approach for supporting accessible, reproducible, and transparent computational research in the life sciences. *Genome Biol* **11**, R86.

Guo, G., Yang, J., Nichols, J., Hall, J. S., Eyres, I., Mansfield, W. and Smith, A. (2009). Klf4 reverts developmentally programmed restriction of ground state pluripotency. *Development* **136**, 1063-1069.

Heinz, S., Benner, C., Spann, N., Bertolino, E., Lin, Y. C., Laslo, P., Cheng, J. X., Murre, C., Singh, H. and Glass, C. K. (2010). Simple combinations of lineage-determining transcription factors prime cis-regulatory elements required for macrophage and B cell identities. *Mol Cell* **38**, 576-589.

Joshi, O., Wang, S. Y., Kuznetsova, T., Atlasi, Y., Peng, T., Fabre, P. J., Habibi, E., Shaik, J., Saeed, S., Handoko, L., et al. (2015). Dynamic Reorganization of Extremely Long-Range Promoter-Promoter Interactions between Two States of Pluripotency. *Cell Stem Cell* **17**, 748-757.

Langmead, B. and Salzberg, S. L. (2012). Fast gapped-read alignment with Bowtie 2. *Nat Methods* **9**, 357-359.

Lawrence, M., Huber, W., Pages, H., Aboyoun, P., Carlson, M., Gentleman, R., Morgan, M. T. and Carey, V. J. (2013). Software for computing and annotating genomic ranges. *PLoS Comput Biol* **9**, e1003118.

Martello, G., Sugimoto, T., Diamanti, E., Joshi, A., Hannah, R., Ohtsuka, S., Gottgens, B., Niwa, H. and Smith, A. (2012). Esrrb is a pivotal target of the Gsk3/Tcf3 axis regulating embryonic stem cell self-renewal. *Cell Stem Cell* **11**, 491-504.

McLean, C. Y., Bristor, D., Hiller, M., Clarke, S. L., Schaar, B. T., Lowe, C. B., Wenger, A. M. and Bejerano, G. (2010). GREAT improves functional interpretation of cis-regulatory regions. *Nat Biotechnol* **28**, 495-501.

Mi, H., Muruganujan, A., Casagrande, J. T. and Thomas, P. D. (2013). Large-scale gene function analysis with the PANTHER classification system. *Nat Protoc* **8**, 1551-1566.

Nowak, D. E., Tian, B. and Brasier, A. R. (2005). Two-step cross-linking method for identification of NF-kappaB gene network by chromatin immunoprecipitation. *Biotechniques* **39**, 715-725.

Ramirez, F., Dundar, F., Diehl, S., Gruning, B. A. and Manke, T. (2014). deepTools: a flexible platform for exploring deep-sequencing data. *Nucleic Acids Res* **42**, W187-191.

Robinson, J. T., Thorvaldsdottir, H., Winckler, W., Guttman, M., Lander, E. S., Getz, G. and Mesirov, J. P. (2011). Integrative genomics viewer. *Nat Biotechnol* **29**, 24-26.

Shechter, D., Dormann, H. L., Allis, C. D. and Hake, S. B. (2007). Extraction, purification and analysis of histones. *Nat Protoc* **2**, 1445-1457.

Trapnell, C., Hendrickson, D. G., Sauvageau, M., Goff, L., Rinn, J. L. and Pachter, L. (2013). Differential analysis of gene regulation at transcript resolution with RNA-seq. *Nat Biotechnol* **31**, 46-53.

Trapnell, C., Pachter, L. and Salzberg, S. L. (2009). TopHat: discovering splice junctions with RNA-Seq. *Bioinformatics* **25**, 1105-1111.

Trapnell, C., Williams, B. A., Pertea, G., Mortazavi, A., Kwan, G., van Baren, M. J., Salzberg, S. L., Wold, B. J. and Pachter, L. (2010). Transcript assembly and quantification by RNA-Seq reveals unannotated transcripts and isoform switching during cell differentiation. *Nat Biotechnol* **28**, 511-515.

Zhang, Z. (2016). Multiple imputation with multivariate imputation by chained equation (MICE) package. *Ann Transl Med* **4**, 30.

Zhu, L. J., Gazin, C., Lawson, N. D., Pages, H., Lin, S. M., Lapointe, D. S. and Green, M. R. (2010). ChIPpeakAnno: a Bioconductor package to annotate ChIP-seq and ChIP-chip data. *BMC Bioinformatics* **11**, 237.